Available online at www.sciencedirect.com

ScienceDirect

Nuclear Physics B 964 (2021) 115330

NUCLEAR PHYSICS B

www.elsevier.com/locate/nuclphysb

TCSA and the finite volume boundary state

Zoltan Bajnok *, Tamas Lajos Tompa

Wigner Research Centre for Physics, Konkoly-Thege Miklós u. 29-33, 1121 Budapest, Hungary

Received 15 December 2020; received in revised form 16 January 2021; accepted 25 January 2021
Available online 29 January 2021
Editor: Hubert Saleur

Abstract

We develop a new way to calculate the overlap of a boundary state with a finite volume bulk state in the truncated conformal space approach. We check this method in the thermally perturbed Ising model analytically, while in the scaling Lee-Yang model numerically by comparing our results to excited state g-functions, which we obtained by the analytical continuation method. We also give a simple argument for the structure of the asymptotic overlap between the finite volume boundary state and a periodic multiparticle state, which includes the ratio of Gaudin type determinants.
© 2021 Wigner Research Centre for Physics. Published by Elsevier B.V. This is an open access article under the CC BY license (http://creativecommons.org/licenses/by/4.0/). Funded by SCOAP[3].

1. Introduction

Recently there have been growing interest in integrable finite volume boundary states and significant progress has been made in the calculation of their overlaps with periodic multiparticle states. This research is fueled by quantum quench problems in statistical physics as well as correlation function calculations in the AdS/CFT duality.

In the AdS/CFT correspondence there are many places where integrable overlaps appeared recently. At first a codimension one defect is introduced in the gauge theory, which allows one-point functions of local gauge invariant operators to be different from zero. These operators correspond to finite volume multiparticle states on the worldsheet and their one-point functions in the presence of the defect can be interpreted as overlaps with a –hopefully integrable– boundary state. There were many perturbative calculations for different subsectors in the D3-D5 [1–3] and

* Corresponding author.
E-mail address: bajnok.zoltan@wigner.hu (Z. Bajnok).

https://doi.org/10.1016/j.nuclphysb.2021.115330
0550-3213/© 2021 Wigner Research Centre for Physics. Published by Elsevier B.V. This is an open access article under the CC BY license (http://creativecommons.org/licenses/by/4.0/). Funded by SCOAP[3].

D3-D7 [4,5] setup and for a few loop orders in the coupling [6,7] together with new developments also in bootstrapping the boundary state and calculating asymptotic overlaps [8–12]. Recently, a new class of three-point functions were investigated involving a local gauge invariant single trace operator and two determinant operators dual to maximal giant gravitons and it was shown to be an overlap between a finite volume multiparticle state and a finite volume integrable boundary state [13,14].

In a statistical physical quench problem there is a sudden change in one of the parameters of the theory. As a result the ground-state of the pre-quenched theory is no longer an eigenstate of the post-quenched one, thus initiates a non-trivial time evolution, which can be integrable [15]. This evolution is relevant to understand if thermalization happens and can be calculated once the overlaps between the (integrable) initial state and multiparticle states are known. The exact overlap results in integrable spin chains [16–18] indicated that non-vanishing overlaps appear for parity symmetric Bethe states only. This was connected to the integrability of the boundary/initial state in [19–21]. There were further progress to calculate time evolutions after a quench from the overlaps in [22–26].

In both applications above the exact knowledge of the overlaps between a finite volume boundary state and periodic multiparticle states is required. Not much is known about these overlaps in quantum field theories for generic excited states. In [27] the first few large volume overlaps were extracted from the investigation of the one-point function. The aim of our paper is twofold. On the one hand we would like to extend these results and describe the finite volume boundary state in terms of the infinite volume characteristics of the theory such as reflection and scattering matrices for any finite size. On the other hand we would like to test these formulas against numerical data obtained from the truncated conformal space approach (TCSA). Although most of the analysis is restricted to the simplest integrable interactive theory, namely to the scaling Lee-Yang model the conceptual ideas and generic form of the results can be easily generalized.

There were already two approaches to calculate excited state overlaps (called g-functions there) from TCSA. The first was concerned with massless flows [28], while the second extracted the g-functions from the evaluation of the partition functions obtained from the finite strip TCSA spectrum [29,30]. Since these approaches seem to be very cumbersome we decided to develop a novel and more direct way of computing the overlaps in the TCSA framework. We test this new method against the large volume scattering description.

Following an old idea, which goes back at least to Lüscher [31,32], it is possible to express finite volume quantities in terms of their infinite volume counterparts. This program was successfully completed for the finite size spectrum, it is under development for finite volume form factors and it can be also carried out for the finite volume boundary state as we will demonstrate in this paper for the scaling Lee-Yang model.

Depending on the nature of the finite size corrections we can distinguish three domains: The leading corrections are polynomial in the inverse of the volume, $O(L^{-1})$, and originate from imposing periodic boundary condition. Characteristic quantities, such as energies and form factors take their infinite volume form, but periodicity implies momentum quantization, which makes the spectrum discrete and changes the natural normalization of states. Subleading corrections are exponentially small in the volume and their leading term, $O(e^{-mL})$, contains a pair of virtual particles which travel around the periodic world [33]. For small enough volumes all virtual processes have to be summed up, which is nicely realized by the Thermodynamic Bethe Ansatz equation for the ground-state [34]. Exact finite volume energies for excited states can be obtained

by analytical continuation [35]. Here assumptions are made for the analytical behavior for the pseudoenergies and the equations obtained are conjectures which have to be tested.

The calculation of the overlap between the finite volume boundary state and the finite volume ground-state called the g-function has a long history. The g-function was first introduced in conformal field theories and characterized the ground-state boundary entropy [36]. Later it was shown to decrease along renormalization group flows similarly to the central charge of CFT [37]. The first attempt to calculate the g-function in massive integrable theories dealt with the evaluation of the partition function with two boundaries in two alternative ways related to each other by exchanging the role of space and time [38]. By evaluating the path integral in the saddle point approximation the boundary condition dependent part of the g-function was correctly calculated. However, the g-function appears as the O(1) piece in the free energy which includes contributions from the quadratic fluctuations as well as from the non-trivial measure in constructing the functional integral [39]. The first result accounting for the full result was obtained in diagonally scattering theories. It was conjectured based on the cluster expansion of the partition function and on attempts to take into account the O(1) contributions [40]. Later, the measure in the path integral was correctly calculated providing the honest derivation of the ground-state g-function [41]. Alternatively, the complete summation of the cluster expansion leads to the same results [42,43]. The authors also tried to extend this approach to excited states' g-functions, however the incorporation of the asymptotic overlaps seemed problematic, although recently improved. This was revealed by an extension of the results for non-diagonal scattering theories and for excited states by analytical continuation in the AdS/CFT setting [13,14]. The aim of our paper is to elaborate further on the calculation of boundary states by analytical continuation and also in the TCSA framework.

The paper is organized as follows: In the next section we recall the infinite volume characterization of integrable boundaries both in space and in time. We then present the polynomial corrections for the boundary state. This will be done after reviewing the same corrections for the spectrum and for form factors. In Section 3 we recall the g-function in diagonally scattering one species models and perform an analytical continuation to obtain the excited states' g-functions together with g-functions in the presence of boundary boundstates. In Section 4 we present our novel proposal for the calculation of excited state g-function in the TCSA framework. We test this proposal in Section 5 for the thermally perturbed Ising model by exact analytical calculations. Section 6 deals with the scaling Lee-Yang model where we compare the novel TCSA results to the numerical evaluation of the TBA g-functions, whose implementation is spelled out in Appendix B. We finally conclude in Section 7 and provide some outlook.

2. The asymptotic boundary state

We first review the two ways how an integrable boundary can be placed in a infinite volume by restricting the 1+1 dimensional space-time into the half plane. We then determine how the infinite volume quantities and momentum quantization can be used to calculate the polynomial corrections to the finite volume boundary state.

2.1. Infinite volume boundary state

An integrable boundary can be placed either in space or in time [44].

2.1.1. Boundary in space, reflections

If the boundary is in space (space is restricted to the negative half-line) boundary conditions can be characterized by reflection factors. The reflection matrix $R_{n\to m}$ is the amplitude of a process in which an asymptotic initial n-particle state consisting of n separated right moving particles reflects into an asymptotic final m-particle state consisting reflected left moving particles. In integrable theories there is no particle creation and the multiparticle reflection factorizes into the product of individual reflections and pairwise scatterings

$$R_{n\to n}(\theta_1,\dots,\theta_n)=\prod_{i<j}S(\theta_i-\theta_j)\prod_{i=1}^{n}R(\theta_i) \tag{2.1}$$

where θ is the rapidity, which parameterizes the relativistic dispersion relation as $(E(\theta),\, p(\theta)) = m(\cosh\theta, \sinh\theta)$. The integrable scattering matrix $S(\theta_1-\theta_2)$ which depends only on the rapidity differences satisfies unitarity and crossing symmetry

$$S(\theta)S(-\theta)=1 \quad ; \qquad S(i\pi-\theta)=S(\theta) \tag{2.2}$$

The reflection factor also satisfies unitarity and boundary crossing symmetry

$$R(\theta)R(-\theta)=1 \quad ; \qquad R(i\pi-\theta)=S(2\theta)R(\theta) \tag{2.3}$$

The origin of the boundary crossing equation seems a bit obscure, but will be clear from the other channel point of view. Once the scattering matrix is specified solutions of the reflection equations characterize integrable boundary conditions in the bootstrap setting. We will analyze two models in this paper, the thermally perturbed Ising model and the scaling Lee-Yang model.

The thermally perturbed Ising model is related to the theory of a free massive fermion and has scattering matrix $S=-1$. The two solutions of the (2.3) bootstrap equations which correspond to fixed/free boundary conditions have the reflection factors

$$R_{\pm}(\theta)=\left(\pm\frac{1}{2}\right)_\theta \quad ; \qquad (x)_\theta=\frac{\sinh(\frac{\theta}{2}+\frac{i\pi x}{2})}{\sinh(\frac{\theta}{2}-\frac{i\pi x}{2})} \tag{2.4}$$

The scaling Lee-Yang model is the only relevant perturbation of the conformal Lee-Yang model and has the scattering matrix [45]

$$S(\theta)=\frac{\sinh\theta+i\sin\frac{\pi}{3}}{\sinh\theta-i\sin\frac{\pi}{3}} \tag{2.5}$$

We will be interested in two reflection factors, which are related to perturbations where only the bulk is perturbed [29]. There are two conformal boundary conditions in the Lee-Yang model labeled by $\mathbb{I}$ and φ. The bulk only perturbation of the identity boundary condition is described by the reflection factor

$$R_{\mathbb{I}}(\theta)=\left(\frac{1}{6}\right)_\theta\left(\frac{1}{2}\right)_\theta\left(-\frac{2}{3}\right)_\theta \tag{2.6}$$

while the perturbation of φ by

$$R_{\varphi}(\theta)=R_{\mathbb{I}}(\theta)\left(\frac{b-1}{6}\right)_\theta\left(\frac{b+1}{6}\right)_\theta\left(\frac{5-b}{6}\right)_\theta\left(-\frac{5+b}{6}\right)_\theta \tag{2.7}$$

with $b=-1/2$. Note that $R_{\mathbb{I}}(\theta)$ can be formally obtained by putting $b=0$. If b is not $-1/2$ then there is also a perturbation at the boundary, but we will not discuss this situation in the paper.

2.1.2. Boundary in time, the boundary state

If the boundary is placed in time it can be characterized as a boundary state [44]. This translation invariant state can be expanded in the basis of the Hilbert space associated to the whole line as

$$|B\rangle = \sum_{n=0}^{\infty} \frac{1}{n!} \prod_i \int \frac{d\theta_i}{4\pi} K_n(\theta_1, \dots, \theta_n) |\theta_1, \dots, \theta_n, -\theta_n, \dots, -\theta_1\rangle \tag{2.8}$$

Infinite volume states are normalized as $\langle\theta|\theta'\rangle = 2\pi\delta(\theta - \theta')$ and integrations go for the whole line. Due to relativistic invariance in the bulk one can relate the boundary state to the multiparticle reflection amplitude as

$$K_n(\theta_1, \dots, \theta_n) = R_{n\to n}(\frac{i\pi}{2} - \theta_1, \dots, \frac{i\pi}{2} - \theta_n) \tag{2.9}$$

Integrability guaranties that only pairs of particles with opposite rapidities appear and the extra $1/2$ in the $1/(4\pi)$ measure reflects this fact. Factorized scattering implies that K_n can be written in terms of the scattering matrix and the reflection factor. Reordering the multiparticle terms shows that the boundary state exponentiates

$$|B\rangle = \exp\{\int \frac{d\theta}{4\pi} K(\theta) Z(-\theta) Z(\theta)\} |0\rangle \tag{2.10}$$

where $Z(\theta)$ is the ZF operator, which creates a particle with rapidity θ and form an exchange algebra

$$Z(\theta_1)Z(\theta_2) = S(\theta_1 - \theta_2) Z(\theta_2) Z(\theta_1) \tag{2.11}$$

while

$$K(\theta) = K_2(\theta) = R(\frac{i\pi}{2} - \theta) \tag{2.12}$$

Consistency of the boundary state implies the relation $K(\theta) = S(2\theta) K(-\theta)$ which is the origin of the boundary crossing unitarity relation. The overlap of an infinite volume multiparticle state with the boundary state is then

$$\langle -\theta_1, \theta_1, \dots, -\theta_n, \theta_n | B\rangle = \prod_{j=1}^{n} K(\theta_i) \tag{2.13}$$

Let us point out that there is a subtlety here. If the reflection factor has a pole at $i\frac{\pi}{2}$, or equivalently if the K- matrix has a pole at $\theta = 0$ of the form

$$K(\theta) = -\frac{ig^2}{2\theta} + \text{regular} \tag{2.14}$$

then the boundary state has a one particle contribution [44,29,46,47]:

$$|B\rangle = \left\{1 + \frac{g}{2} Z(0)\right\} \exp\left\{ \fint \frac{d\theta}{4\pi} K(\theta) Z(-\theta) Z(\theta) \right\} |0\rangle \tag{2.15}$$

with a principal value integration. This one-particle term has a drastic effect on the finite size energy corrections on the strip [48] and on boundary form factors [49], and also shows up in the overlaps with odd number of particles (containing a standing particle):

$$\langle -\theta_1, \theta_1, \dots, -\theta_n, \theta_n, 0 | B\rangle = \frac{g}{2} \prod_{j=1}^{n} K(\theta_i) \tag{2.16}$$

2.2. Polynomial corrections to the finite volume boundary state

In the following we give a simple argument for the form of the asymptotic finite volume boundary state. We start by recalling the similar corrections for the energy spectrum and also for form factors.

2.2.1. Leading finite size corrections for the spectrum and for form factors

As we already mentioned in the introduction we express all finite volume quantities in terms of their infinite volume analogues. Putting N particles in a finite volume L the momentum is quantized by the Bethe-Yang (BY) equations

$$Q_j = p(\theta_j)L - i\sum_{k:k\neq j}\log S(\theta_j-\theta_k) = 2\pi n_j \tag{2.17}$$

Once the quantization numbers $\{n_j\}$ are specified the rapidities $\{\theta_j\}$ can be calculated. For large volumes the free quantization dominates $p(\theta_i) = \frac{2\pi n_i}{L}$ and the scattering interaction introduces polynomial corrections in L^{-1}. The energy of the state containing all of these polynomial corrections is formally the same as in infinite volume

$$E(n_1,\dots,n_N) = \sum_j E(\theta_j) + O(e^{-mL}) \tag{2.18}$$

but the momenta are quantized by the BY equations.

We now recall the leading finite size correction of the form factor [50,51], which is the matrix element of a local operator $\mathcal{O}$ between asymptotic states:

$$F_N^{\mathcal{O}}(\theta_1,\dots,\theta_N) = \langle 0|\mathcal{O}|\theta_1,\dots,\theta_N\rangle \tag{2.19}$$

This state is originally defined for strictly ordered rapidities, $\theta_i > \theta_{i+1}$, but can be generalized via $|\theta_1,\dots,\theta_i,\theta_{i+1}\dots,\theta_N\rangle = S(\theta_i-\theta_{i+1})|\theta_1,\dots,\theta_{i+1},\theta_i,\dots,\theta_N\rangle$ for any orderings. The normalization is

$$\langle\theta'_N,\dots,\theta'_1|\theta_1,\dots,\theta_N\rangle = (2\pi)^N\prod_{i=1}^N\delta(\theta_i-\theta'_i) + \text{permutations} \tag{2.20}$$

where permutations contain terms obtained by exhanging θs all possible ways and by picking up the corresponding S-matrix factors.

The finite volume state can be characterized either by the quantization numbers $\{n_i\}$ or by the corresponding rapidities $\{\theta_i\}$. We denote this state as $|n_1,\dots,n_N\rangle_L \equiv |\theta_1,\dots,\theta_N\rangle_L$, which is typically symmetric for the exchanges of particles. Since the finite volume spectrum is discrete the natural normalization is

$${}_L\langle n'_1,\dots,n'_N|n_1,\dots,n_N\rangle_L = \prod_i \delta_{n'_i n_i} \tag{2.21}$$

We emphasize that it is not the same as the infinite volume normalization, which can be easily seen by relating them for large volumes. In doing so we compare the resolution of the identity

$$\sum_{N=0}^{\infty}\sum_{\{n_i\}}|n_1,\dots,n_N\rangle_L\,{}_L\langle n_N,\dots,n_1| = \mathbb{I} = \sum_{N=0}^{\infty}\prod_i\int\frac{d\theta_i}{2\pi}|\theta_1,\dots,\theta_N\rangle\langle\theta_N,\dots,\theta_1| \tag{2.22}$$

The two operators on the two sides of the equation act in different Hilbert spaces, however for large volumes the rapidities become spaced as dense as $\frac{2\pi}{L}$. The very dense rapidity space summation for the N particles states then can be replaced with integration

$$\sum_{\{n_i\}} |\{n_i\}\rangle_{L\ L}\langle\{n_i\}| = \prod_i \int \frac{d\theta_i}{2\pi} \rho_N(\{\theta_j\}) |\theta_1, \dots, \theta_N\rangle_{L\ L}\langle\theta_N, \dots, \theta_1| \tag{2.23}$$

where the density of states is the Jacobian of changing variables from $\{n_j\}$ to $\{\theta_j\}$ via the BY equations:

$$\rho_N(\{\theta_j\}) = \det \left| \frac{\partial Q_j}{\partial \theta_i} \right| = \det \begin{vmatrix} p_1' L + \phi_{12} + \dots \phi_{1N} & \dots & -\phi_{1N} \\ \vdots & \ddots & \vdots \\ -\phi_{N1} & \dots & p_N' L + \phi_{N1} + \dots + \phi_{NN-1} \end{vmatrix} \tag{2.24}$$

where $p'(\theta) = \frac{dp(\theta)}{d\theta}$ and $\phi_{jk} = \phi(\theta_j - \theta_k) = -i\partial_{\theta_j} \log S(\theta_j - \theta_k)$. We can now compare the integrands for each particle numbers' integrations leading to the relation between finite and infinite volume normalizations [51]

$$|\theta_1, \dots, \theta_N\rangle_L = \frac{|\theta_1, \dots, \theta_N\rangle}{\sqrt{\prod_{i<j} S(\theta_i - \theta_j) \rho_N(\theta_1, \dots, \theta_N)}} + O(e^{-mL}) \tag{2.25}$$

Clearly the phase of the state cannot be fixed in this way, it follows from demanding a symmetric finite volume state. We note that the relation does not rely on large particle numbers, merely on large volumes, and is valid even for one or two particle states.

The finite volume form factor up to exponentially small corrections is basically the infinite volume form factor modulo the change in the normalization of states:

$$\langle 0|\mathcal{O}|\theta_1, \dots, \theta_N\rangle_L = \frac{F_N^{\mathcal{O}}(\theta_1, \dots, \theta_N)}{\sqrt{\prod_{i<j} S(\theta_i - \theta_j) \rho_N(\theta_1, \dots, \theta_N)}} + O(e^{-mL}) \tag{2.26}$$

as was obtained from comparing the infinite and finite volume 2-point functions in [51]. Let us use this normalization change to calculate the finite volume boundary state.

2.2.2. *Leading finite size correction for the boundary state*

The finite volume boundary state can be expressed in the basis of the finite volume Hilbert space with periodic boundary condition in the form:

$$|B\rangle_L = |B\rangle_L^{\text{even}} + |B\rangle_L^{\text{odd}} \tag{2.27}$$

where we separated the contribution of the parity symmetric BY states for containing even and odd number of particles. The odd term $|B\rangle_L^{\text{odd}}$ is nonzero only if $\text{res}_{\theta=0} K(\theta) \neq 0$. We spell out this term in Appendix A. In the following we assume that this term is absent and write simply

$$|B\rangle_L = \sum_N \sum_{\{n_j\}} K_N(n_1, \dots, n_N)_L |n_1, \dots, n_N, -n_N, \dots, -n_1\rangle_L \tag{2.28}$$

Similarly how we related the resolution of the identity for large volumes we can also replace the summation for pairs of particles for integrations of those pairs. In doing so we have to use the relation

$$Q_j^- = p(\theta_j)L - i\sum_{k:k\neq j}\log S(\theta_j-\theta_k) - i\sum_k \log S(\theta_j+\theta_k) = 2\pi n_j \tag{2.29}$$

and change variable from $\{n_j\}$ to $\{\theta_j\}$. The corresponding Jacobian is $\rho_N^- = \det\left|\frac{\partial Q_j^-}{\partial\theta_i}\right|$. Additionally we also express the finite volume state in terms of the infinite volume state and arrive at

$$|B\rangle_L = \sum_N \prod_i \int \frac{d\theta_i}{4\pi} K_N(\theta_1,\dots,\theta_N)_L \frac{\rho_N^-}{\sqrt{\prod_i S(-2\theta_i)\rho_{2N}}} |-\theta_1,\theta_1,-\theta_2,\theta_2,\dots,-\theta_N,\theta_N\rangle \tag{2.30}$$

Here we note that the correct way of calculating the norm of the state is to move a bit away from the pairwise structure and take the appropriate limit. This can be easily done by introducing one single extra particle and sending its rapidity to infinity. What is important is that we have to consider θ and $-\theta$ independent when calculating the derivatives and substitute their pairwise structure into the general ρ_{2N}. Actually ρ_{2N} for pairwise states $\{\theta_1,\dots,\theta_N,-\theta_1,\dots,-\theta_N\}$ factorizes as

$$\rho_{2N} = \det\begin{vmatrix} A & B \\ B & A \end{vmatrix} = \det\begin{vmatrix} A-B & B \\ 0 & A+B \end{vmatrix} = \rho_N^-\rho_N^+ \tag{2.31}$$

where $\rho_N^\pm$ are obtained from ρ_N by replacing $\phi_{ij} = \phi(\theta_i-\theta_j)$ with $\phi_{ij}^\pm = \phi(\theta_i-\theta_j)\pm\phi(\theta_i+\theta_j)$. By comparing this expression with the infinite volume boundary state (2.8) we arrive at the relation

$$\begin{aligned} K_N(\theta_1,\dots,\theta_N)_L &= \frac{\sqrt{\rho_{2N}}}{\sqrt{\prod_i S(2\theta_i)\rho_N^-}}\prod_i K_2(\theta_i) + O(e^{-mL}) \\ &= \prod_i \frac{K_2(\theta_i)}{\sqrt{S(2\theta_i)}}\sqrt{\frac{\rho_N^+}{\rho_N^-}} + O(e^{-mL}) \end{aligned} \tag{2.32}$$

where we assumed that, similarly to the spectrum and form factors, we have no other polynomial volume effects. The first few terms of this expression was obtained from the analysis of the 1-point function in [27] and the structure was proven for simple spin chains in [52]. Our argumentations could be extended for integrable spin chains, if one could show that the boundary state in the thermodynamic limit has the form (2.8). Note that the finite volume boundary state is a symmetric even function of the rapidities. We will confirm this result by calculating the exact finite volume expressions and taking the large volume limit.

3. Exact finite volume boundary state

In this section we recall the derivation of the exact finite volume g-functions. We then review how to extend the result for excited states by analytical continuation.

The finite volume groundstate overlap is called the g-function, which can be obtained from the evaluation of the partition function on the cylinder [38], see Fig. 3.1. Depending on which time evolution we choose there are two representations of the partition function

$$Z_{\alpha\beta}(L,R) = {}_L\langle B_\beta|e^{-H(L)R}|B_\alpha\rangle_L = \mathrm{Tr}(e^{-H_{\alpha\beta}(R)L}) \tag{3.1}$$

By evolving for a very large Euclidean time, $R\to\infty$, only the periodic groundstate survives

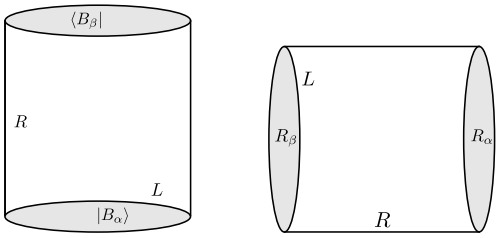

Fig. 3.1. Two alternative ways to calculate the partition function depending on the chosen time evolution.

$$\lim_{R\to\infty} Z_{\alpha\beta}(L,R) = {}_L\langle B_\beta|0\rangle\langle 0|B_\alpha\rangle_L e^{-E_0(L)R} + \dots \tag{3.2}$$

allowing for a direct extraction of the g-function $g_\alpha(L) = \langle 0|B_\alpha\rangle_L$ as

$$\log(g_\alpha(L)g_\beta(L)) = \lim_{R\to\infty}\left\{R^{-1}\log Z_{\alpha\beta}(L,R) + E_0(L)\right\} \tag{3.3}$$

The idea is to calculate this quantity in the other channel, where the volume is large and polynomial corrections are enough to be kept:

$$Z_{\alpha\beta}(L,R) = \mathrm{Tr}(e^{-H_{\alpha\beta}(R)L}) = \sum_n e^{-E^n_{\alpha\beta}(R)L} \tag{3.4}$$

here n labels multiparticle state on the strip. These polynomial corrections come from momentum quantization with reflections on the two ends and scatterings among the particles:

$$2\pi n_k = 2mR\sinh\theta_k - i\log R_\alpha(\theta_k) - i\log R_\beta(\theta_k) - i\sum_{j:j\neq k}\log\left\{S(\theta_k-\theta_j)S(\theta_k+\theta_j)\right\} \tag{3.5}$$

The energy is

$$E^n_{\alpha\beta}(R) = \sum_{k=1}^n m\cosh\theta_k + f_\alpha + f_\beta \tag{3.6}$$

where f_α and f_β are the boundary energies, which are typically normalized to 0 in the TBA setting. Recently there were developments in summing up directly the contributions of the multiparticle states in the cluster expansion [42]. This can be done by introducing non-linear integral equations for the diagrammatic evaluation of the contributions. Alternatively, the traditional way is to introduce densities of states and turn the sum for multiparticle states into a functional integral for the densities [38]. Since the g-function is the O(1) term in the partition function special care needs to be taken for constructing the measure of the integral as well as for evaluating the quadratic fluctuations [39–41].

3.1. Groundstate g-function

The outcome of this analysis is that the g-function can be written as

$$g_\alpha(L)g_\beta(L) = \frac{\det(1-K^-)}{\det(1-K^+)}\times \exp\left\{\int\frac{d\theta}{4\pi}\left(\phi_\alpha(\theta)+\phi_\beta(\theta)-2\phi(2\theta)-2\pi\delta(\theta)\right)\log(1+e^{-\epsilon(\theta)})\right\} \tag{3.7}$$

where $\phi_{\alpha/\beta}(\theta) = -i\,\partial_\theta \log R_{\alpha/\beta}(\theta)$ and $\epsilon(\theta)$ is the solution of the TBA equation

$$\epsilon(\theta) = mL\cosh\theta - \int \frac{d\theta'}{2\pi}\phi(\theta-\theta')\log(1+e^{-\epsilon(\theta')}) \tag{3.8}$$

for the groundstate energy

$$E_0^{\mathrm{TBA}}(L) = -m\int \frac{d\theta}{2\pi}\cosh\theta\log(1+e^{-\epsilon(\theta)}) \tag{3.9}$$

on the circle of size L. The Fredholm operators $K^\pm$ are defined by their integral kernels:

$$K^\pm f(\theta) = \int_0^\infty \frac{d\theta'}{2\pi}\frac{\phi^\pm(\theta,\theta')}{1+e^{\epsilon(\theta)}} f(\theta') \quad ; \qquad \phi^\pm(\theta,\theta') = \phi(\theta-\theta') \pm \phi(\theta+\theta') \tag{3.10}$$

The numerator in the ratio of Fredholm determinants comes from the fluctuations, while the denominator is related to the non-trivial measure in the functional integral [41,53].

3.2. Groundstate g-function with boundary boundstates

This formula is valid if there are no boundary boundstates. In some cases it can happen that the physical boundary condition characterized by $R_\alpha(\theta)$ has a boundary boundstate say at iu:

$$R_\alpha(\theta) = i\frac{g_\alpha^2}{2(\theta-iu)} + \text{regular} \tag{3.11}$$

In this case the g-function takes the form [30]

$$g_\alpha(L) = \sqrt{\frac{\det(1-K^-)}{\det(1-K^+)}}(1+e^{-\epsilon(iu)})\exp\left\{\int\frac{d\theta}{4\pi}\left(\phi_\alpha(\theta)-\phi(2\theta)-\pi\delta(\theta)\right)\log(1+e^{-\epsilon(\theta)})\right\} \tag{3.12}$$

This term can be understood as an analytical continuation from a domain where there are no boundary boundstates. During the continuation the pole of ϕ_α crosses the integration contour, whose contribution has to be picked up. The g-function without this contribution corresponds to the boundary boundstate. For more than one boundstates all of their contributions $\prod_j(1+e^{-\epsilon(iu_j)})$ have to be included.

3.3. Excited states g-function

We can analytically continue the ground-state equations in order to describe excited states. In doing so singularities $\bar\theta_i$, related to the particles' rapidities, θ_i, cross the integration contour and introduce extra source terms [35]. For the energy they contribute as

$$E_n^{\mathrm{TBA}}(L) = im\sum_j \eta_j \sinh\bar\theta_j - m\int\frac{d\theta}{2\pi}\cosh\theta\,\log(1+e^{-\epsilon(\theta)}) \tag{3.13}$$

where ϵ satisfies the excited state TBA equation

$$\epsilon(\theta) = mL\cosh\theta + \sum_j \eta_j \log S(\theta-\bar\theta_j) - \int\frac{d\theta'}{2\pi}\phi(\theta-\theta')\log(1+e^{-\epsilon(\theta')}) \tag{3.14}$$

and the parameters η_j keep track of the location of the poles. For poles on the upper half plane $\eta_j = 1$, while for those on the lower half plane $\eta_j = -1$. The position of the singularities is related to the zeros of the logarithm of $1 + e^{-\epsilon}$:

$$\epsilon(\bar{\theta}_k) = i\pi(2n_k + 1) \tag{3.15}$$

For free fermions and for the sinh-Gordon model $\bar{\theta}_k = \theta_k + i\frac{\pi}{2}$, while for the scaling Lee-Yang model each particle is represented by a complex conjugate pair of rapidities $\bar{\theta}_k = \theta_k + i\delta_k$ and $\bar{\theta}_{k+n} = \theta_k - i\delta_k$, where for large volumes δ_k approaches $\pi/6$. The excited states g-functions are the overlaps between the finite volume boundary state and periodic finite volume multiparticle states

$$g_\alpha(\{n_k\}, L) = \sqrt{\frac{\det(1 - K_{\rm ex}^-)}{\det(1 - K_{\rm ex}^+)}} \prod_k \frac{R_\alpha(\bar{\theta}_k)}{\sqrt{S(2\bar{\theta}_k)}} \times \exp\left\{ \int \frac{d\theta}{4\pi} (\phi_\alpha(\theta) - \phi(2\theta) - \pi\delta(\theta)) \log(1 + e^{-\epsilon(\theta)}) \right\} \tag{3.16}$$

where the Fredholm operators have a discrete and a continuous part [54,55]:

$$K_{\rm ex}^\pm \cdot \begin{pmatrix} f(\bar{\theta}_j) \\ f(\theta') \end{pmatrix} = \begin{pmatrix} K_k^\pm(\bar{\theta}_j) & K^\pm(\bar{\theta}_k, \theta') \\ K_j^\pm(\theta) & K^\pm(\theta, \theta') \end{pmatrix} \begin{pmatrix} f(\bar{\theta}_j) \\ f(\theta') \end{pmatrix} \tag{3.17}$$

where

$$K_k^\pm(\theta) = \frac{\phi^\pm(\bar{\theta}_k, \theta)}{-i\partial_\theta \epsilon(\theta)|_{\bar{\theta}_k}} \quad ; \qquad K^\pm(\theta, \theta') = \frac{\phi^\pm(\theta, \theta')}{1 + e^{\epsilon(\theta')}} \tag{3.18}$$

It is easy to see in the sinh-Gordon and free fermion cases that $R_\alpha(\theta + \frac{i\pi}{2})/\sqrt{S(i\pi + 2\theta)} = K(\theta)/\sqrt{S(2\theta)}$. It was shown in [13,14] that the large volume limit of $\det(1 - K_{\rm ex}^\pm)$ goes to $\det \rho^\mp$ thus the exact result reproduces correctly the asymptotic form (2.32).

For the free fermion the kernel vanishes, $\phi(\theta) = 0$, and the exact overlaps take the form

$$g_\alpha(\{n_k\}, L) = \prod_k i K_\alpha(\theta_k) \exp\left\{ \int \frac{d\theta}{4\pi} (\phi_\alpha(\theta) - \pi\delta(\theta)) \log(1 + e^{-mL\cosh(\theta)}) \right\} \tag{3.19}$$

For the scaling Lee-Yang model we elaborate on the numerical evaluations of the overlaps in Appendix B as these will be compared to the same quantities obtained from TCSA, which is the topic of the next section.

4. Overlaps in the TCSA framework

In this section we propose a new way to "measure" the overlaps between the finite volume boundary state and the finite volume multiparticle states in the TCSA framework.

4.1. TCSA for the energy

The truncated conformal space approach is a very efficient variational approximation, which was originally developed for relevant perturbations of conformal field theories in order to calculate their finite size energy spectrum on the circle [56]. The Hamiltonian of the perturbed system can be written as

$$H = H_0 + \lambda \int_0^L \Phi(x,t)dx \quad ; \qquad H_0 = \frac{2\pi}{L}(L_0 + \bar{L}_0 - \frac{c}{12}) \tag{4.1}$$

where c is the central charge of the CFT, while the Virasoro generators L_0 and $\bar{L}_0$ act diagonally on the Virasoro highest weight representations $\mathcal{V}_i$, $\bar{\mathcal{V}}_i$ from which the Hilbert space is built up[1] as

$$\mathcal{H} = \sum_i \mathcal{V}_i \otimes \bar{\mathcal{V}}_i \tag{4.2}$$

By mapping the cylinder onto the plane, $(x + iy \to z = e^{-i\frac{2\pi}{L}(x+iy)} = re^{i\theta})$, the Hamiltonian takes the form

$$H = \frac{2\pi}{L}\left[L_0 + \bar{L}_0 - \frac{c}{12} + \lambda \left(\frac{L}{2\pi}\right)^{2-2h} 2\pi \int_0^{2\pi} \frac{d\theta}{2\pi}\, \Phi(e^{i\theta}, e^{-i\theta}) \right] \tag{4.3}$$

where h is the chiral weight of the spinless perturbation. The θ integration implies momentum conservation. Typically, when we calculate the matrix elements of Φ, we choose the Virasoro basis in each Verma module and ensure that singular vectors are eliminated. This basis is not orthogonal and the inner product matrix, G, can be calculated from the defining relations of the Virasoro algebra. The idea of TCSA is to truncate the conformal Hilbert space at a given energy E_{cut}, and to diagonalize numerically the Hamiltonian

$$\frac{H}{m} = \frac{2\pi}{mL}\left(L_0 + \bar{L}_0 - \frac{c}{12} + \left(\frac{mL}{2\pi\kappa}\right)^{2-2h} 2\pi\, G^{-1}\Phi \right) \tag{4.4}$$

at the given truncation, where

$$m = \kappa \lambda^{\frac{1}{2-2h}} \tag{4.5}$$

is a mass parameter, typically chosen to be the massgap. The eigenvalues $E_n(L)$ of the Hamiltonian are the finite volume energy levels of multiparticle states, while the eigenvectors $|n,\lambda\rangle_L$ are their representations on the conformal Hilbert space. These vectors then can be used to calculate finite volume form factors[2] [51] and, as we will show, also finite volume overlaps.

Alternatively one can also do perturbation theory with the Hamiltonian

$$H = H_0 + \lambda L^{1-2h} V \tag{4.6}$$

This is called conformal perturbation theory (CPT) and for the groundstate energy it gives

$$E_0(L,\lambda) = -\frac{\pi c}{6L} + \lambda \langle \text{vac}|V(L)|\text{vac}\rangle + \cdots = -\frac{\pi c}{6L} + L^{-1}\sum_{k=1}^{\infty} (\lambda L^{2-2h})^k b_k \tag{4.7}$$

while for the groundstate eigenvector

$$|\text{vac},\lambda\rangle_L = |\text{vac}\rangle + \lambda L^{2-2h} \sum_{n\neq \text{vac}} c_n |n\rangle + \dots \quad ; \qquad c_n L = \frac{\langle n|V|\text{vac}\rangle}{\langle \text{vac}|H_0|\text{vac}\rangle - \langle n|H_0|n\rangle} \tag{4.8}$$

[1] Here we assume diagonal modular invariant partition functions.

[2] TCSA can be used to calculate boundary form factors as well [57,58].

where $|\text{vac}\rangle$ denotes the lowest energy state of the conformal field theory. The perturbative expansion of the groundstate energy indicates that it is normalized differently than the groundstate energy in the TBA setting

$$E_0(L,\lambda) = E_0^{\text{TBA}}(L) + f_{\text{bulk}} L \tag{4.9}$$

the difference being the vacuum energy density.

4.2. Conformal boundary conditions

In a conformal field theory we can also place a boundary in two different ways [45]. A space boundary is conformal, if there is no energy flow through the boundary: $T_{xy}|_{x=0} = 0$. In holomorphic coordinates it reads as $T(z)|_{x=0} = \bar{T}(\bar{z})|_{x=0}$, which implies that the symmetry is no longer the tensor product of two Virasoro algebras, rather it is one single Virasoro algebra. Boundary conditions can be labeled by representations of the chiral algebra, such that on the strip with boundary conditions α and β representations of the fusion product of α and β appear only in the decomposition of the Hilbert space

$$\mathcal{H}_{\alpha\beta} = \sum_i N^i_{\alpha\beta} \mathcal{V}_i \tag{4.10}$$

where $N^i_{\alpha\beta}$ are the Verlinde fusion numbers which can be calculated from the modular $\mathcal{S}$-matrix.

If however the boundary is in time it is represented as an initial or final state, $|B\rangle$, which can be expanded in the basis of the periodic Hilbert space, obtained by mapping the boundary onto the plane. Conformal invariance translates into the condition

$$(L_n - \bar{L}_{-n})|B\rangle = 0 \tag{4.11}$$

These conformal states, called Ishibashi states, are unique for each highest weight representation $\mathcal{V}_i \otimes \bar{\mathcal{V}}_i$ and can be constructed as follows: We choose the basis in each chiral half by Virasoro descendants including only linearly independent combinations

$$|i\rangle = L_{-n_1} \dots L_{-n_k}|h\rangle \quad ; \qquad \langle i| = \langle h|L_{n_k} \dots L_{n_1} \tag{4.12}$$

Their inner product matrix follows from the Virasoro algebra and will be denoted as

$$\langle i|j\rangle = M_{ij} \quad ; \qquad M^{ij} M_{jk} = \delta^i_k \tag{4.13}$$

The Ishibashi state can be written simply in terms of the inverse of this inner product matrix as

$$|h\rangle\rangle = M^{ik}|i\rangle \otimes |\bar{k}\rangle \tag{4.14}$$

where $|\bar{k}\rangle$ is obtained from $|k\rangle$ by replacing L with $\bar{L}$.

Space and time boundaries can be connected by conformal transformations. Specific boundary conditions in space, labeled by representations, do not correspond directly to Ishibashi states. They are related to Cardy states $|B_\alpha\rangle$, which are linear combinations of Ishibashi states

$$|B_\alpha\rangle = \sum_i g^i_\alpha |h_i\rangle\rangle \tag{4.15}$$

The coefficients can be fixed by demanding that the cylinder partition function, calculated in the two alternative time evolutions, are the same. We normalize the Ishibashi states as

$$\langle\langle h_j|e^{-H_0 R}|h_i\rangle\rangle = \delta_{ij}\langle h_i|h_i\rangle \chi_i(q) \tag{4.16}$$

Time evolution by the strip Hamiltonian $H_{\text{strip}}(R) = \frac{\pi}{R}(L_0 - \frac{c}{24})$ on the Hilbert space $\mathcal{H}_{\alpha\beta}$ leads to Cardy's condition

$$g^i_\alpha g^i_\beta \langle i|i\rangle = \sum_j N^j_{\alpha\beta} \mathcal{S}^i_j \tag{4.17}$$

where $\mathcal{S}$ is the matrix which represents the modular transformation on the characters. This equation can be solved, which provides the physical, Cardy, boundary states [59].

4.3. TCSA for boundary states and overlaps

In the following we analyze theories which are perturbed in the bulk but not at the boundaries. The perturbed theory is a massive scattering theory, which in the integrable case can be characterized by the mass of the particle and by its scattering matrix. If the boundary is in space these particles reflect off it and the boundary condition is characterized by the reflection matrix. If however the boundary is in time then it is characterized by its overlap with the bulk multiparticle states. In the case when there is no boundary perturbation it is natural to assume that the boundary state does not change[3] and we can calculate the overlap as the overlap between the conformal boundary state, i.e. the Cardy state, and the normalized multiparticle state, $|n, \lambda\rangle$, represented on the conformal Hilbert space either by TCSA or by CPT. Thus we define the overlap in the deformed theory for the vacuum as

$$g^{\text{TCSA}}_\alpha(L) = \langle \text{vac}, \lambda | B_\alpha \rangle \tag{4.18}$$

By comparing the small coupling/volume perturbative formulas [30] we can conclude that it is normalized differently than the g-function in the TBA setting. They differ by a term linear in the volume, which is proportional to the boundary energy f_α:

$$\log g^{\text{TCSA}}_\alpha(L) = \log g_\alpha(L) - f_\alpha L \tag{4.19}$$

The excited states overlap, which can be compared to the TBA results are simply

$$\log g_\alpha(n, L) = \log\langle n, \lambda | B_\alpha \rangle + f_\alpha L \tag{4.20}$$

In the following we test this idea analytically in the thermally perturbed Ising model and numerically in the scaling Lee-Yang model.

5. Free massive fermion

The critical Ising model can be described by the $c = \frac{1}{2}$ CFT which has three representations $h = 0$, $h = \frac{1}{2}$ and $h = \frac{1}{16}$. Its spinless perturbation with the $h = \frac{1}{2}$ field corresponds to moving away from the critical temperature. This model is equivalent to free massive fermions of mass m, which can be solved exactly providing an ideal framework to test our proposal for the overlaps.

[3] If in the bulk-boundary OPEs of the bulk perturbing operator there are singularities, one might need to renormalize the boundary state.

5.1. Free massless fermion

Let us first describe the CFT in terms of free massless (Euclidean) fermions

$$i\psi(z) = \sum_n b_n z^{-n-\frac{1}{2}} \quad ; \qquad \{b_n, b_m\} = \delta_{n+m} \tag{5.1}$$

They can be either periodic, Neveu-Schwartz sector, with half integer modes or anti-periodic, Ramond sector, with integer modes. The Virasoro algebra is represented in the NS sector as

$$L_n = \sum_{j>\frac{n}{2}} (j - \frac{n}{2}) b_{n-j} b_j \quad ; \qquad j \in \mathbb{N} + \frac{1}{2} \tag{5.2}$$

In the Ramond sector we simply take $j \in \mathbb{N}$ and for $j = 0$

$$L_0 = \sum_{j>0} j b_{-j} b_j + \frac{1}{4} b_0^2 \quad ; \qquad b_0^2 = \frac{1}{2} \tag{5.3}$$

There are analogous formulas for the other chiral fermion $\bar{\psi}(\bar{z})$ in terms of $\bar{b}_n$. The NS vacuum, $|0\rangle$, corresponds to the identity representation of the Virasoro algebra, while the $h = \frac{1}{2}$ representation to $b_{-\frac{1}{2}} \bar{b}_{-\frac{1}{2}} |0\rangle$. The Ramond vacuum is nothing but the $h = \frac{1}{16}$ highest weight state. In the following we work with periodic boundary condition and take the free Hamiltonian

$$H_0 = \frac{2\pi}{L}(L_0 + \bar{L}_0 - \frac{c}{12}) = \frac{2\pi}{L}(\sum_{n>0} n b_{-n} b_n + \sum_{n>0} n \bar{b}_{-n} \bar{b}_n - \frac{1}{24}) \tag{5.4}$$

in the NS sector.

5.2. Mass perturbation

We then add the relevant spinless perturbation on the cylinder which corresponds to the mass term

$$H = H_0 + mV \quad ; \qquad V = -\frac{i}{2\pi} \int_0^L \psi \bar{\psi} dx \tag{5.5}$$

By mapping the perturbation onto the plane we get the perturbation in terms of fermion modes:

$$V = i \left(\frac{2\pi}{L}\right)^{2h-1} \int \frac{d\theta}{2\pi} \sum_{n,k} b_n \bar{b}_k e^{i\theta(n-k)} = i \sum_n b_n \bar{b}_n \tag{5.6}$$

The nth mode Hilbert space with basis $\{|0\rangle, b_{-n}|0\rangle, \bar{b}_{-n}|0\rangle, b_{-n}\bar{b}_{-n}|0\rangle\}$ is left invariant by the perturbation, thus we can simply diagonalize the corresponding 4 by 4 matrix. Since the momentum

$$P_0 = \frac{2\pi}{L}(L_0 - \bar{L}_0) = \frac{2\pi}{L}(\sum_{n>0} n b_{-n} b_n - \sum_{n>0} n \bar{b}_{-n} \bar{b}_n) \tag{5.7}$$

commutes with the perturbed Hamiltonian and it has eigenvalues $\{0, k_n, -k_n, 0\}$ with $k_n = 2n\pi/L$, only the zero momentum vectors $|0\rangle$ and $b_{-n}\bar{b}_{-n}|0\rangle$ are mixed. As a result the eigenvalues are $\{k_n - \omega_n, k_n, k_n, k_n + \omega_n\}$ with $\omega_n = \sqrt{m^2 + k_n^2}$ and the energy differences account

correctly for the free relativistic spectrum of mass m. Clearly the interacting vacuum is a complicated object in the conformal Hilbert space as it is entangled between all the modes. The easiest way to describe this vacuum is to introduce new creation-annihilation operators with a given momentum eigenvalue k_n for $n > 0$:

$$\beta_n = b_n + \gamma_n \bar{b}_{-n} \quad ; \qquad \beta_n^\dagger = b_{-n} + \gamma_n^\star \bar{b}_n \tag{5.8}$$

and similarly with momentum $-k_n$:

$$\beta_{-n} = \alpha_n b_{-n} + \bar{b}_n \quad ; \qquad \beta_{-n}^\dagger = \alpha_n^\star b_n + \bar{b}_{-n} \tag{5.9}$$

These operators are not normalized properly, rather they are written in the form, such that in the $m \to 0$ limit both $\alpha_n \to 0$ and $\gamma_n \to 0$ and we get back the conformal result. By demanding the free fermion form for the Hamiltonian

$$H = \sum_{n>0} \left\{ \rho_n (\beta_n^\dagger \beta_n + \beta_{-n}^\dagger \beta_{-n}) + \kappa_n \right\} \tag{5.10}$$

together with the independence of the modes $\{\beta_n, \beta_{-n}\} = 0$ we can find the following solution

$$\rho_n = \frac{m}{2} e^{\theta_n} \quad ; \qquad \alpha_n = -ie^{-\theta_n} \quad ; \quad \gamma_n = ie^{-\theta_n} \quad ; \qquad \kappa_n = -me^{-\theta_n} \tag{5.11}$$

where we introduced the rapidity as $k_n = m \sinh \theta_n$. The norms of the states are related to

$$\{\beta_n^\dagger, \beta_n\} = 1 + |\gamma_n|^2 = 1 + e^{-2\theta_n} \quad ; \qquad \{\beta_{-n}^+, \beta_{-n}\} = 1 + |\alpha_n|^2 = 1 + e^{-2\theta_n} \tag{5.12}$$

In order to obtain the new vacuum $|0, m\rangle$ we demand that

$$\beta_n |0, m\rangle = \beta_{-n} |0, m\rangle = 0 \tag{5.13}$$

Such state can easily be constructed as

$$|0, m\rangle \propto \prod_{n>0} \beta_{-n} \beta_n |0\rangle \propto \prod_{n>0} (1 + \alpha_n b_{-n} \bar{b}_{-n}) |0\rangle = \prod_{n>0} (1 - ie^{-\theta_n} b_{-n} \bar{b}_{-n}) |0\rangle \tag{5.14}$$

We might normalize this state by dividing with $\mathcal{N} = \prod_{n>0} \sqrt{1 + e^{-2\theta_n}}$:

$$|0, m\rangle = \mathcal{N}^{-1} \prod_{n>0} (1 - ie^{-\theta_n} b_{-n} \bar{b}_{-n}) |0\rangle$$

Excited states are obtained by acting with the creation operators. They act non-trivially in their own mode numbers and that factor of the product is modified as

$$\beta_n^\dagger |0, m\rangle \propto b_{-n} |0\rangle \quad ; \qquad \beta_{-n}^\dagger |0, m\rangle \propto \bar{b}_{-n} |0\rangle \quad ; \qquad \beta_n^\dagger \beta_{-n}^\dagger |0, m\rangle \propto (e^{-\theta_n} + ib_{-n} \bar{b}_{-n}) |0\rangle \tag{5.15}$$

Thus the normalized two particle state with zero momentum and mode number k is

$$|\{k\}, m\rangle = \mathcal{N}^{-1} (e^{-\theta_k} + ib_{-k} \bar{b}_{-k}) \prod_{n \neq k} (1 - ie^{-\theta_n} b_{-n} \bar{b}_{-n}) |0\rangle \tag{5.16}$$

Let us elaborate on the groundstate energy. In the perturbed picture the groundstate energy is

$$E_0(L) = \sum_{n>0} \kappa_n = -\sum_{n>0} (\omega_n - k_n) \tag{5.17}$$

which is nothing but the sum of the zero point fluctuation energies compared to the same expression without the perturbation. This expression is expected to be written as

$$E_0(L) = f_{\text{bulk}} L + E_0^{\text{TBA}}(L) = f_{\text{bulk}} L - m \int \frac{d\theta}{2\pi} \cosh\theta \, \log(1 + e^{-mL\cosh\theta}) \tag{5.18}$$

however f_{bulk} is infinite and needs regularization. We will face a similar divergence also for the overlaps.

5.3. Conformal boundary conditions and overlaps

We now turn to the description of conformal boundary conditions in the fermionic language. The Cardy states in the Ising model can be written in terms of the Ishibashi states as [45]

$$\begin{aligned}
|B_0\rangle &= \frac{1}{\sqrt{2}}|0\rangle\rangle + \frac{1}{\sqrt{2}}|\tfrac{1}{2}\rangle\rangle + \frac{1}{\sqrt[4]{2}}|\tfrac{1}{16}\rangle\rangle \\
|B_{\frac{1}{2}}\rangle &= \frac{1}{\sqrt{2}}|0\rangle\rangle + \frac{1}{\sqrt{2}}|\tfrac{1}{2}\rangle\rangle - \frac{1}{\sqrt[4]{2}}|\tfrac{1}{16}\rangle\rangle \\
|B_{\frac{1}{16}}\rangle &= |0\rangle\rangle - |\tfrac{1}{2}\rangle\rangle
\end{aligned} \tag{5.19}$$

As we are focusing on the NS sector we distinguish two boundary states $|B_\pm\rangle = |0\rangle\rangle \pm |\frac{1}{2}\rangle\rangle$. Let us see how they can be described in the fermionic language. Boundary states in the free fermion algebra are defined by

$$(b_n \pm i\bar{b}_{-n})|B\rangle = 0 \tag{5.20}$$

and the sign reflects the fixed or the free boundary conditions. Since the inner product matrix is diagonal in the fermionic basis the Ishibashi states are diagonal, too. The fermionic boundary condition also fixes how we combine the Ishibashi states of $|0\rangle\rangle$ and $|\frac{1}{2}\rangle\rangle$:

$$|B_\pm\rangle = e^{\pm i \sum_n b_{-n}\bar{b}_{-n}}|0\rangle = \prod_n e^{\pm i b_{-n}\bar{b}_{-n}}|0\rangle = \prod_n (1 \pm i b_{-n}\bar{b}_{-n})|0\rangle \tag{5.21}$$

Clearly this state satisfies (5.20) and the Ishibashi condition but it is not normalized.

Let us note that in the UV limit, $m \to 0$, the interacting vacuum goes to the conformal vacuum $|0, m\rangle \to |0\rangle$, while in the IR limit, $m \to \infty$ the rapidities all go to zero and $|0, m\rangle \to |B_-\rangle$ as was observed in [60].

The boundary state $|B_\pm\rangle$ in the basis of the nth mode $\{|0\rangle, b_{-n}|0\rangle, \bar{b}_{-n}|0\rangle, b_{-n}\bar{b}_{-n}|0\rangle\}$ takes a very simple form $\{1, 0, 0, \pm i\}$.

Now we are ready to test our proposal for the overlaps. Following our suggestion the finite volume overlap of the boundary state with the groundstate can be calculated as

$$g_\pm^{\text{TCSA}}(L) = \langle 0, m|B_\pm\rangle = \prod_n \frac{1 \mp e^{-\theta_n}}{\sqrt{1 + e^{-2\theta_n}}} \tag{5.22}$$

As the boundary states are not normalizable and the boundary energies f_α are infinite [30,40] (just as the bulk energy) a better quantity is the ratio of the groundstate and excited state overlaps. The overlap of an excited state consisting a pair of particles with vanishing total momentum is:

$$g_\pm^{\text{TCSA}}(\{k\}, L) = \langle\{k\}, m|B_\pm\rangle = \frac{e^{-\theta_k} \pm 1}{\sqrt{1 + e^{-2\theta_k}}} \prod_{n\neq k} \frac{1 \mp e^{-\theta_n}}{\sqrt{1 + e^{-2\theta_n}}} \tag{5.23}$$

The ratio of the two quantities is

$$\frac{g_{\pm}^{\mathrm{TCSA}}(\{k\}|L)}{g_{\pm}^{\mathrm{TCSA}}(L)} = \frac{e^{-\theta_k} \pm 1}{1 \mp e^{-\theta_k}} = \begin{cases} \frac{e^{-\theta_k}+1}{1-e^{-\theta_k}} = \coth\frac{\theta_k}{2} \\ -\frac{1-e^{-\theta_k}}{1+e^{-\theta_k}} = -\tanh\frac{\theta_k}{2} \end{cases} \tag{5.24}$$

Recall that in the block notation the reflection factor for the + boundary is

$$R_+(\theta) = \left(\frac{1}{2}\right)_\theta \quad ; \qquad K_+(\theta) = R_+(\frac{i\pi}{2}+\theta) = i\coth\frac{\theta}{2} \tag{5.25}$$

while for the − boundary we have

$$R_-(\theta) = \left(-\frac{1}{2}\right)_\theta \quad ; \qquad K_-(\theta) = R_-(\frac{i\pi}{2}+\theta) = -i\tanh\frac{\theta}{2} \tag{5.26}$$

and they agree with the exact results (3.19) up to a sign, which can be defined into the normalization of the excited states.

Thus we are convinced that the overlap in the massive theory can be calculated in the TCSA framework as the matrix element of the conformal boundary state with the massive scattering state, which is realized on the conformal Hilbert space.

6. Scaling Lee-Yang model

In the Lee-Yang model the central charge is $c = -\frac{22}{5}$ and we have just two irreducible representations with $h = 0$ and $h = -\frac{1}{5}$. The Hilbert space is built over the two highest weight spinless fields: $\mathbb{I}$ and the other which we denote by Φ as $\mathcal{H} = \mathcal{V}_0 \otimes \bar{\mathcal{V}}_0 + \mathcal{V}_{-\frac{1}{5}} \otimes \bar{\mathcal{V}}_{-\frac{1}{5}}$. This is a non-unitary theory and the state with the lowest energy is $|\mathrm{vac}\rangle = |\Phi\rangle$. The conformal Hamiltonian on the strip is simply

$$H_0 = \frac{2\pi}{L}(L_0 + \bar{L}_0 - \frac{c}{12}) \tag{6.1}$$

and we perturb it with the only relevant spinless field Φ as (4.4). In order to keep the g-functions and the structure constant real it is advantageous to take the normalization $\langle 0|0\rangle = -1$ and $\langle\Phi|\Phi\rangle = 1$. This leads to the matrix elements

$$\langle\Phi|\Phi|\Phi\rangle = \sqrt{\frac{2}{1+\sqrt{5}}}\frac{\Gamma(\frac{1}{5})\Gamma(\frac{6}{5})}{\Gamma(\frac{3}{5})\Gamma(\frac{4}{5})} \quad ; \qquad \langle\Phi|\Phi|0\rangle = \langle 0|\Phi|\Phi\rangle = 1 \tag{6.2}$$

The perturbation results in a massive scattering theory of a single particle type, whose mass is related to the coupling (4.5) as

$$\kappa = 2^{\frac{19}{12}}\sqrt{\pi}\frac{\left(\Gamma(\frac{3}{5})\Gamma(\frac{4}{5})\right)^{\frac{5}{12}}}{5^{\frac{5}{16}}\Gamma(\frac{2}{3})\Gamma(\frac{5}{6})} = 2.642944... \tag{6.3}$$

In comparing the TCSA spectrum with those coming from TBA we note that the bulk energy constant is

$$f_{\mathrm{bulk}} = -\frac{1}{4\sqrt{3}}m^2 \tag{6.4}$$

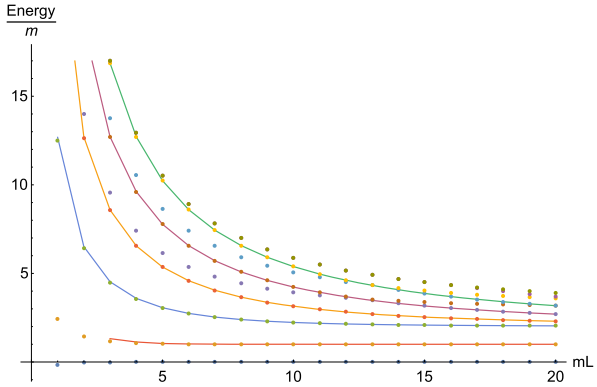

Fig. 6.1. TCSA energy spectrum with bulk energy subtracted in the zero momentum sector. The first state is the vacuum, the second is a standing one particle state, while the next two are moving two-particle states. Higher levels cross each other, for instance the fifth energy level can be a 2- or a 3- particle scattering state depending on the volume. Continuous lines indicate 2-particle Bethe-Yang lines with quantum numbers $n = 0, \dots, 4$.

There are two physical boundary conditions corresponding to the representations $h = 0$ and $h = -\frac{1}{5}$ labeled by $\mathbb{I}$ and φ, respectively. The related Cardy states can be expressed in terms of the Ishibashi states as [29]

$$|B_{\mathbb{I}}\rangle = -\left(\frac{1}{2} + \frac{1}{2\sqrt{5}}\right)^{\frac{1}{4}} |0\rangle\rangle + \left(\frac{1}{2} - \frac{1}{2\sqrt{5}}\right)^{\frac{1}{4}} |-\tfrac{1}{5}\rangle\rangle \tag{6.5}$$

$$|B_{\varphi}\rangle = \left(1 - \frac{2}{\sqrt{5}}\right)^{\frac{1}{4}} |0\rangle\rangle + \left(1 + \frac{2}{\sqrt{5}}\right)^{\frac{1}{4}} |-\tfrac{1}{5}\rangle\rangle \tag{6.6}$$

The corresponding reflection factors are (2.6), (2.7), see [29], while the boundary energies are

$$f_{\mathbb{I}} = \frac{1}{4}(\sqrt{3} - 1)m \quad ; \qquad f_{\varphi} = f_{\mathbb{I}} - m \sin\frac{\pi}{12} \tag{6.7}$$

In implementing TCSA for the Lee-Yang model we generated the periodic Hilbert space (4.2) with energy cuts ranging from 10 to 18 in the chiral Verma modules and diagonalized the truncated Hamiltonian (4.4) numerically. The low lying spectrum with the bulk energy subtracted is presented in Fig. 6.1. The two particle Bethe-Yang lines

$$Q(\theta_n) = mL \sinh\theta_n - i \log S(2\theta_n) = 2\pi n \quad ; \qquad E_n(L) = 2m \cosh\theta_n \tag{6.8}$$

are plotted for $n = 0, \dots, 4$. The state with $n = 0$ is actually a 1-particle state, which can be interpreted as a boundstate for $mL > 3$. Having obtained the spectrum together with the corresponding eigenvalues we calculated their overlaps with the boundary states (6.5) constructed on the truncated Hilbert space. In the following we report on the comparison of the outcome of these TCSA overlap calculations (4.18), (4.20) against various available results for small (UV), large (IR) and intermediate (TBA) volumes. We investigate in details the first four eigenstates, which includes the finite volume vacuum, a 1-particle state and two 2-particle states.

6.1. Small volume checks of TCSA overlaps

For small volumes we can compare the TCSA results with CPT calculations. The groundstate g-function has the expansion

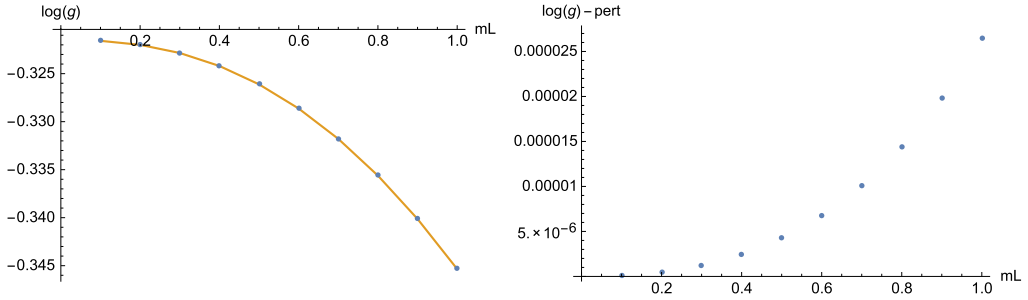

Fig. 6.2. Comparison of TCSA and conformal perturbation theory (6.9). On the left: TCSA data points for $\log(g_{\mathbb{I}}^{\mathrm{CFT}})$ are plotted against the dimensionless volume $mL = 0.1, \ldots, 1$ with dots and conformal perturbation theory up to d_4 with a continuous line. The difference of the two is shown on the right, indicating the next order polynomial correction.

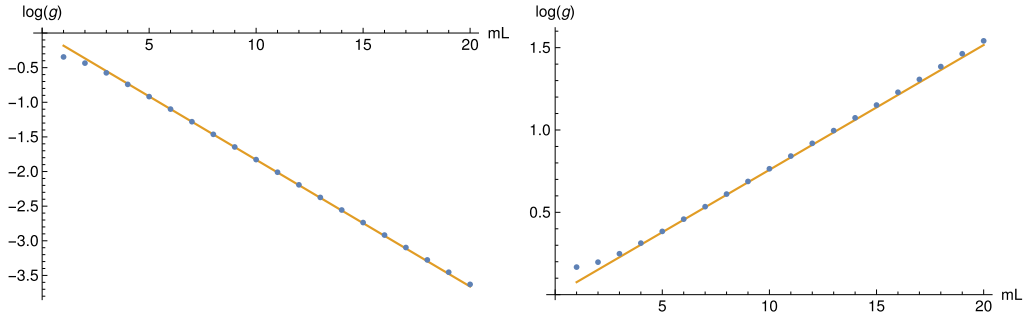

Fig. 6.3. The overlap of the vacuum with the boundary states. On the left, logarithm of the overlap between the vacuum and the identity boundary state (dots) is plotted against the dimensionless volume together with $-f_{\mathbb{I}}\, mL$ (continuous line). On the right the overlap with the φ boundary and $-f_{\varphi} mL$.

$$\log g_{\mathbb{I}}^{\mathrm{CFT}} = \log {}_L\langle \mathrm{vac}, \lambda | B_{\mathbb{I}} \rangle = \frac{1}{4} \log \left(\frac{1}{2} + \frac{1}{2\sqrt{5}} \right) + \sum_{i=1}^{\infty} d_i (mL^{\frac{12}{5}}/\kappa)^i \tag{6.9}$$

where conformal perturbation theory gives the following coefficients [30,40]:

$$d_1 = -0.25312 \quad ; \qquad d_2 = 0.0775 \quad ; \qquad d_3 = -0.0360 \quad ; \qquad d_4 = 0.0195 \tag{6.10}$$

In Fig. 6.2 we compare the TCSA results with the CPT calculations and find complete agreement. This confirms that the coefficients and signs coming from various square-roots in the boundary state are implemented correctly[4] and give us confidence to move on to the large volume analysis.

6.2. *Large volume checks of TCSA overlaps*

Let us start with the vacuum overlaps. In Fig. 6.3 the logarithm of (4.18) is plotted as a function of the dimensionless volume mL for both boundary conditions. Clearly the TCSA overlaps (4.19) contain the boundary energies (6.7). In the following we subtract these linear contributions from the logarithm of the overlaps and analyze only the difference. In doing so we can observe stronger

[4] Note that some of our signs in the boundary state are different from [30], which can be related to different conventions.

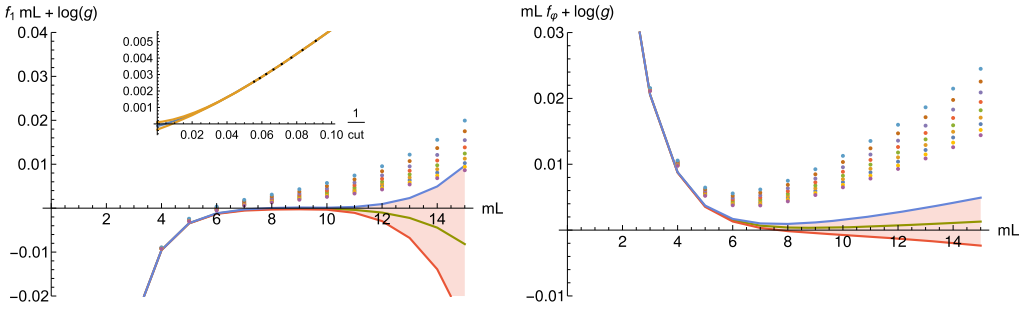

Fig. 6.4. The difference between the logarithm of the overlap and the boundary energy, $\log g_{\mathbb{I}}^{\mathrm{CFT}} + f_{\mathbb{I}}\, mL$, for various cuts ranging from 10 to 18 on the left. TCSA data are plotted with dots, such that higher cuts are closer to zero. Extrapolated results with 90% confidence range are plotted with solid lines. The inset shows the extrapolation in the cut for $mL = 10$. Similar plots for the φ boundary are on the right.

dependence on the cut. We then introduce an (conservative) extrapolation for each volume in the cut of the form

$$(g_{\mathbb{I}}^{\mathrm{CFT}})|_{\mathrm{cut}} = (g_{\mathbb{I}}^{\mathrm{CFT}})|_{\infty} + \frac{b}{\mathrm{cut}} + \frac{c}{\mathrm{cut}^2} + \frac{d}{\mathrm{cut}^{\frac{12}{5}}} + \frac{e}{\mathrm{cut}^3} \tag{6.11}$$

where *cut* is the truncation level of the chiral Virasoro Verma modules. The extrapolated results, presented in Fig. 6.4, show both that the extrapolation is correct and that the logarithm of the TBA normalized g-functions vanishes for large volumes. In the next subsection we compare these extrapolated results to TBA calculations.

We next analyze the overlaps with a standing one particle state. Since both reflection factors have a pole at $i\pi/2$ with residues

$$R_\alpha(\theta) = i\frac{g_\alpha^2}{2\theta - i\pi} + \dots \quad ; \quad g_{\mathbb{I}} = 2\sqrt{2\sqrt{3}-3} \quad ; \quad g_\varphi = \sqrt{2}\sqrt[4]{3}\sin^2\left(\frac{\pi}{8}\right)\csc^2\left(\frac{5\pi}{24}\right) \tag{6.12}$$

the leading finite size correction takes the form (A.7):

$$\log {}_L\langle 1,\lambda|B_\alpha\rangle + f_\alpha mL = \frac{g_\alpha}{2}\sqrt{\tilde{\rho}_1^+} + O(e^{-mL}) = \frac{g_\alpha}{2}\sqrt{mL} + O(e^{-mL}) \tag{6.13}$$

The asymptotic form of the overlaps with two particle states takes the form

$$\begin{aligned}\log {}_L\langle 2,\lambda|B_\alpha\rangle + f_\alpha mL &= \frac{K_\alpha(\theta)}{\sqrt{S(2\theta)}}\sqrt{\frac{\rho_1^+(\theta)}{\rho_1^-(\theta)}} + O(e^{-mL}) \\ &= \frac{R_\alpha(\frac{i\pi}{2}-\theta)}{\sqrt{S(2\theta)}}\sqrt{\frac{p'(\theta)L}{p'(\theta)L + 2\phi(2\theta)}} + O(e^{-mL})\end{aligned} \tag{6.14}$$

where for any volume L the rapidity θ is determined from the quantization condition (6.8). The TCSA overlap calculations for the first 4 states are compared to the asymptotic expressions in Figs. 6.5 and 6.6. Clearly we find a convincing evidence.

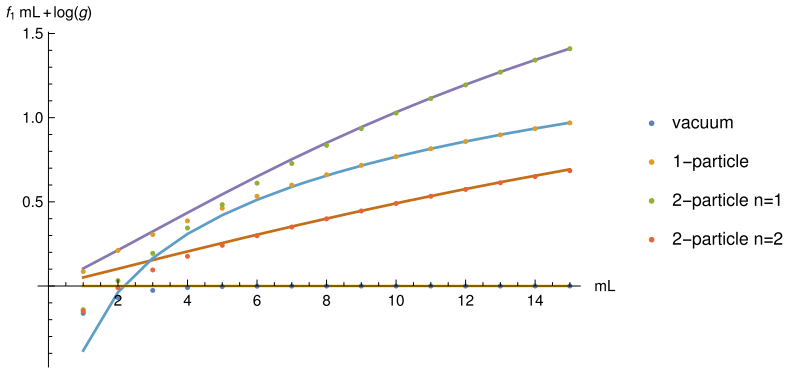

Fig. 6.5. The expression $\log {}_L\langle n,\lambda|B_{\mathbb{I}}\rangle + f_{\mathbb{I}}mL$ is plotted for the first four states with dots. These include the vacuum, the 1-particle state and two 2-particle states with quantization numbers $n = 1, 2$ in (6.8). The asymptotic expressions are plotted with solid lines. The extrapolation errors are negligible on the plot.

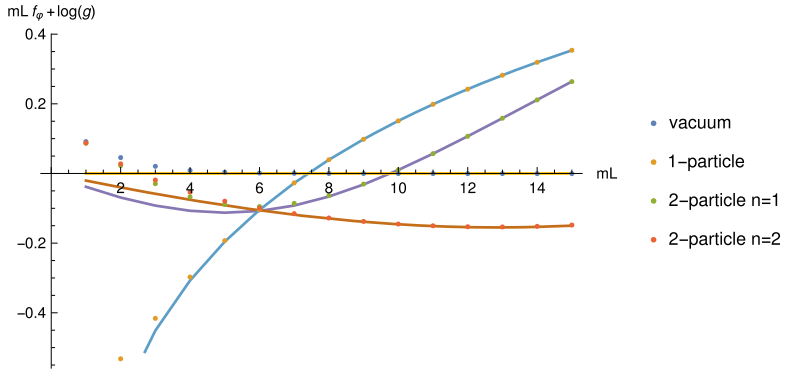

Fig. 6.6. The expression $\log {}_L\langle n,\lambda|B_{\varphi}\rangle + f_{\varphi}mL$ is compared for the first four states including the vacuum, the 1-particle state and two 2-particle states with quantization numbers $n = 1, 2$ to the asymptotic expressions (solid lines).

6.3. TBA checks against TCSA at intermediate volume

Finally, we compare the TCSA data against the solutions of the TBA equations. We start with the groundstate expression.

$$g_{\mathbb{I}}(L) = \sqrt{\frac{\det(1-K^-)}{\det(1-K^+)}}\exp\left\{\int\frac{d\theta}{4\pi}\left(\phi_{\mathbb{I}}(\theta)-\phi(2\theta)-\pi\delta(\theta)\right)\log(1+e^{-\epsilon(\theta)})\right\} \tag{6.15}$$

We explain in Appendix B how to evaluate this expression numerically. The comparison is shown on the left of Fig. 6.7.

Interestingly the φ boundary has a boundary boundstate so the g-function takes the form [30]

$$g_{\varphi}(L) = \sqrt{\frac{\det(1-K^-)}{\det(1-K^+)}}(1+e^{-\epsilon(i\pi/12)})\times \\ \exp\left\{\int\frac{d\theta}{4\pi}\left(\phi_{\varphi}(\theta)-\phi(2\theta)-\pi\delta(\theta)\right)\log(1+e^{-\epsilon(\theta)})\right\} \tag{6.16}$$

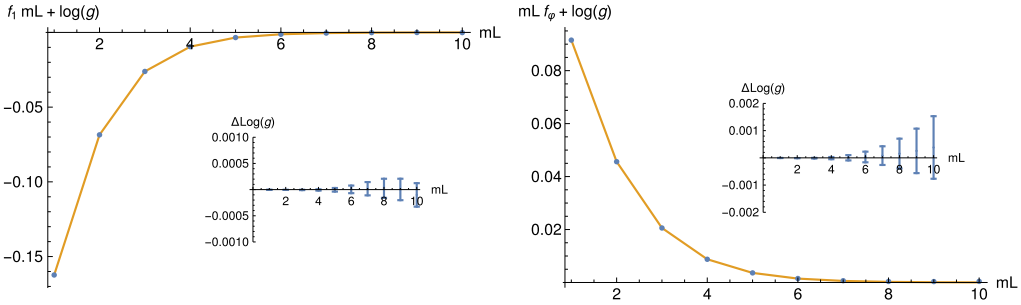

Fig. 6.7. The logarithm of the groundstate g-functions calculated numerically from TBA equations is plotted with solid lines against extrapolated TCSA with dots for the identity boundary condition on the left while for φ on the right. The insets enlarge the differences of the two.

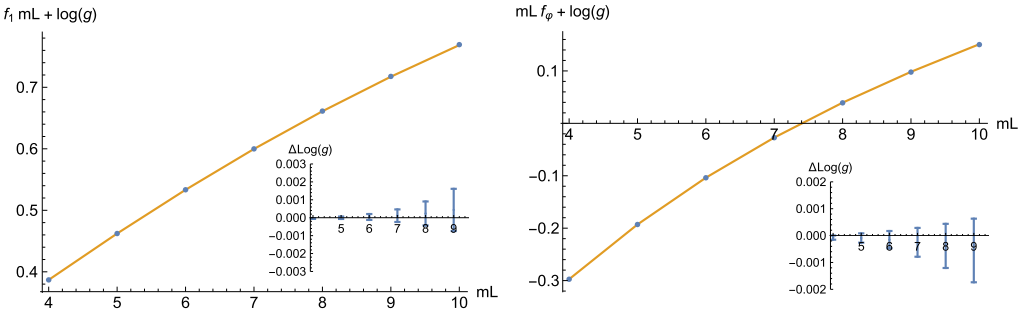

Fig. 6.8. The 1-particle g-functions calculated numerically from TBA equations are plotted with solid lines against extrapolated TCSA with dots for the identity boundary condition on the left while for φ on the right.

This is confirmed by comparing the TBA results to TCSA on the right of Fig. 6.7.

A standing one particle state is obtained by analytical continuation and takes the following form for the identity boundary

$$g_{\mathbb{I}}(\{0\},L) = \sqrt{\frac{\det(1-K_{\rm ex}^{-})}{\det(1-K_{\rm ex}^{+})}}\,\frac{R_{\mathbb{I}}(\bar\theta_1)}{\sqrt{S(2\bar\theta_1)}}\times \\ \exp\left\{\int\frac{d\theta}{4\pi}\,(\phi_{\mathbb{I}}(\theta)-\phi(2\theta)-\pi\delta(\theta))\log(1+e^{-\epsilon(\theta)})\right\} \tag{6.17}$$

In Appendix B we spell out the details how we calculated all the ingredients of this expression numerically. In the case of the φ boundary we have to include additionally the contribution of the boundary boundstate:

$$g_{\varphi}(\{0\},L) = \sqrt{\frac{\det(1-K_{\rm ex}^{-})}{\det(1-K_{\rm ex}^{+})}}\,\frac{R_{\varphi}(\bar\theta_1)}{\sqrt{S(2\bar\theta_1)}}(1+e^{-\epsilon(i\pi/12)})\times \\ \exp\left\{\int\frac{d\theta}{4\pi}\,\big(\phi_{\varphi}(\theta)-\phi(2\theta)-\pi\delta(\theta)\big)\log(1+e^{-\epsilon(\theta)})\right\} \tag{6.18}$$

The comparison of these two cases is shown in Fig. 6.8. We note that the excited state TBA equation has a solution only for $mL > 3$ in the form of (3.14).

In summarizing, we can say that in all the investigated cases we found convincing agreement between the TBA, TCSA and CPT results.

7. Conclusions

The aim of our paper was to elaborate on the finite volume boundary state. In doing so we first provided a simple argument to explain the structure of the asymptotic overlaps. In order to focus on the conceptual issues we presented the ideas for the simplest integrable theories having a single particle type only. We showed that neglecting exponentially small finite size corrections the overlap contains the product of infinite volume overlaps/reflection factors and the square root of the ratio of two determinants originating from the normalization of finite volume states. We then analyzed carefully the analytical continuation of the ground-state g-function in the scaling Lee-Yang theory and obtained excited state g-functions. In order to test these formulas we developed a new way of calculating finite volume overlaps in TCSA. Assuming the absence of boundary perturbations in the Lagrangian description it is simply the overlap of the conformal boundary state with the eigenstate of the TCSA Hamiltonian. We tested this idea with explicit calculations in the thermally perturbed Ising model aka the free massive fermion. In the scaling Lee-Yang model our results confirm completely the excited state g-functions obtained by analytical continuation. In particular for the φ boundary, which has a boundary boundstate, we confirm [30] that the g-function has a factor signaling this boundstate. Additionally we presented a numerical implementation for the solutions of the various TBA equations and the calculations of the overlaps.

Thorough the paper we assumed that the boundary is not perturbed only the bulk. It would be very tempting to extend the analysis for boundary perturbations. In doing so the bulk-boundary operator product expansion could be used to represent the boundary perturbations in the bulk as an operator dressing the conformal boundary state.

We chose the Lee-Yang model to test our ideas as the implementation of the TCSA method is probably the simplest. Recent developments however in TCSA make it possible to apply the method for the sinh-Gordon theory [61,62] where the extension of the TBA results [63] for excited states could be checked.

Here we analyzed only diagonally scattering theories. It would very interesting to extend and test these techniques for non-diagonal scatterings. Then results such as [64] could be tested. Also challenging is the calculation of the g-functions for the $O(N)$ models, where results from [65] can be relevant.

CRediT authorship contribution statement

Z. Bajnok: Conceptualization, Methodology, Software, Formal analysis, Writing draft, Visualization, Supervision, Funding acquisition.

T.L. Tompa: Software, Formal analysis.

Declaration of competing interest

The authors declare that they have no known competing financial interests or personal relationships that could have appeared to influence the work reported in this paper.

Acknowledgements

We thank Gerard Watts, Anatoly Konechny, Stephan Fredenhagen, Maté Lencsés, Balázs Pozsgay, Márton Kormos, Gábor Takács and Tamás Gombor for the useful discussions and comments, the NKFIH research Grants K116505, K134946 and UK_Gyak for supports.

Appendix A. The generic finite volume boundary state

The finite volume boundary state can be expressed in the basis of the finite volume Hilbert space with periodic boundary condition in the form:

$$|B\rangle_L = |B\rangle_L^{\text{even}} + |B\rangle_L^{\text{odd}} \tag{A.1}$$

where we already calculated the even part in the bulk of the paper. In the following we assume that $\text{res}_{\theta=0} K(\theta) \neq 0$ and calculate the odd part, which contains a standing particle

$$|B\rangle_L^{\text{odd}} = \sum_N \sum_{\{n_j\}} K_N^{\text{odd}}(0, n_1, \dots, n_N)_L |n_1, \dots, n_N, 0, -n_N, \dots, -n_1\rangle_L \tag{A.2}$$

Similarly how we related the resolution of the identity for large volumes we can also replace the summation for pairs of particles for integration of those pairs. In doing so we have to use the relation

$$Q_j^{\text{odd}} = p(\theta_j)L - i\log S(\theta_j) - i\sum_{k:k\neq j} \log S(\theta_j - \theta_k) - i\sum_k \log S(\theta_j + \theta_k) = 2\pi n_j \tag{A.3}$$

and change variable from $\{n_j\}$ to $\{\theta_j\}$. The corresponding Jacobian is $\rho_N^{\text{odd}} = \det\left|\frac{\partial Q_j^{\text{odd}}}{\partial \theta_i}\right|$. Additionally, we also express the finite volume state in terms of the infinite volume state and arrive at

$$|B\rangle_L^{\text{odd}} = \sum_N \prod_i \int \frac{d\theta_i}{4\pi} K_N^{\text{odd}}(0, \theta_1, \dots, \theta_N)_L \frac{\rho_N^{\text{odd}}}{\sqrt{\prod_i S(-2\theta_i)\rho_{2N+1}}} \times |0, -\theta_1, \theta_1, -\theta_2, \theta_2, \dots, -\theta_N, \theta_N\rangle \tag{A.4}$$

In calculating ρ_{2N+1} for states of the form $\{\theta_1, \dots, \theta_N, 0, -\theta_1, \dots, -\theta_N\}$ we have the following factorization [66]

$$\rho_{2N+1} = \det\begin{vmatrix} A & b & B \\ b & a & b \\ B & b & A \end{vmatrix} = \det\begin{vmatrix} A-B & 0 & 0 \\ b & a & 2b \\ B & b & A+B \end{vmatrix} = \rho_N^{\text{odd}} \bar{\rho}_{N+1}^{+} \tag{A.5}$$

where $a = mL + 2\sum_{j=1}^N \phi_j$ with $\phi_j = \phi(\theta_j)$ while the jth component of the vector b is $b_j = -\phi_j$. For completeness we spell out that

$$A_{ij} = \delta_{ij}(p_i' L + \phi_j + \sum_k \phi_{ik}) - \phi_{ij} \quad ; \qquad B_{ij} = -\phi(\theta_i + \theta_j) \tag{A.6}$$

with $\phi_{ij} = \phi(\theta_i - \theta_j)$, thus one can easily see that $\det|A - B| = \rho_N^{\text{odd}}$. By comparing this expression with the infinite volume boundary state we arrive at the relation

$$K_N^{\rm odd}(\theta_1,\dots,\theta_N)_L = \frac{\sqrt{\rho_{2N+1}}}{\sqrt{\prod_i S(2\theta_i)}\rho_N^{\rm odd}}\frac{g}{2}\prod_i K_2(\theta_i) + O(e^{-mL})$$
$$= \frac{g}{2}\prod_i \frac{K_2(\theta_i)}{\sqrt{S(2\theta_i)}}\sqrt{\frac{\bar\rho^+_{N+1}}{\rho_N^{\rm odd}}} + O(e^{-mL}) \tag{A.7}$$

The first few terms of this expression agree with [24].

Appendix B. Numerical solution of the TBA equations and overlaps

In this Appendix we explain how we solve numerically the TBA equations and calculate the g-functions.

B.1. Groundstate

In the following we present a numerical approach to the overlaps. The real θ line will be discretized into N points θ_i with distance $\theta_{i+1}-\theta_i = d\theta$, such that the label of the origin is $i0$: $\theta_{i0}=0$. Each function $f(\theta)$ is then represented by a vector $f_i = f(\theta_i)$ while the kernel in the integration by a matrix

$$\phi_{ij} = \frac{d\theta}{2\pi}\phi(\theta_i-\theta_j) \tag{B.1}$$

The groundstate TBA equation is a vector equation of the form

$$\epsilon_i = mL\cosh\theta_i - \sum_j \phi_{ij}\log(1+e^{-\epsilon_j}) \tag{B.2}$$

This can be solved by Findroot in Mathematica or by iterations. The groundstate energy is

$$E_0(L)/m = -\frac{d\theta}{2\pi}\sum_i \cosh\theta_i \log(1+e^{-\epsilon_i}) \tag{B.3}$$

For the calculation of the g-function we introduce the matrices

$$K^{\pm}_{ij} = \frac{d\theta}{2\pi}\frac{\phi(\theta_i-\theta_j)\pm\phi(\theta_i+\theta_j)}{1+e^{\epsilon_i}} \tag{B.4}$$

for indices when both $\theta_i,\theta_j>0$. The saddle point value of the g-function is

$$\log g_\alpha = -\frac{1}{4}\log(1+e^{-\epsilon_{i0}}) + \frac{d\theta}{4\pi}\sum_i(\phi_\alpha(\theta_i)-\phi(2\theta_i))\log(1+e^{-\epsilon_i})$$
$$+\frac{1}{2}\left(\log\det(\mathbb{I}-K^-)-\log\det(\mathbb{I}-K^+)\right) \tag{B.5}$$

where $\phi_\alpha = -i\partial_\theta \log R_\alpha(\theta)$ and the contribution of the measure and fluctuations can be easily calculated in terms of finite matrices in any program say in Mathematica.

In case of a boundary boundstate at iu we add a term

$$\log(1+e^{-\epsilon_u}) \quad ; \qquad \epsilon_u = mL\cos u - \sum_j \phi(iu-\theta_j)\log(1+e^{-\epsilon_j})$$

B.2. Excited states

For simplicity we analyze a standing one-particle state in the Lee-Yang model. This means two singularities at $\bar\theta_1 = i\delta_1$ and $\bar\theta_2 = -i\delta_1$. We denote $\bar\theta_1$ by $\theta_{\bar 1}$. The idea is to extend functions and kernels with extra components at $\bar\theta_1$: $f_{\bar 1} = f(\bar\theta_1)$ and $\phi_{\bar 1 j} = \phi(\bar\theta_1 - \theta_j)$. In particular the TBA equations take the form

$$\epsilon_i = mL\cosh\theta_i + \log\frac{S(\theta_i-\theta_{\bar 1})}{S(\theta_i+\theta_{\bar 1})} - \sum_j \phi_{ij}\log(1+e^{-\epsilon_j}) \tag{B.6}$$

$$0 = mL\cosh\theta_{\bar 1} - \log S(2\theta_{\bar 1}) - \sum_j \phi_{\bar 1 j}\log(1+e^{-\epsilon_j})$$

One can solve these equations by iterations starting from $\epsilon_i = 0$ and $\theta_{\bar 1} = i(\pi/6 + \sqrt{3}e^{-mL\cos(\pi/6)})$. Once $\theta_{\bar 1}$ and ϵ_i are obtained the energy is

$$E(\{0\},L)/m = 2i\sinh\theta_{\bar 1} - \frac{d\theta}{2\pi}\sum_i \cosh\theta_i\log(1+e^{-\epsilon_i}) \tag{B.7}$$

In calculating the excited state g-function the saddle point contribution has the previous form, but there is an extra contribution from $\theta_{\bar 1}$:

$$\log\frac{R_{\mathbb{I}}(\theta_{\bar 1})}{\sqrt{S(2\theta_{\bar 1})}} \tag{B.8}$$

Finally the kernels $K^{\pm}$ have to be extended also with the discrete mode to have $K^{\pm}_{\rm ex}$:

$$K^{\pm}_{\bar 1\bar 1} = \frac{i}{\partial\epsilon_{\bar 1}}\phi^{\pm}_{\bar 1\bar 1} \quad ; \qquad K^{\pm}_{j\bar 1} = \frac{i}{\partial\epsilon_{\bar 1}}\phi^{\pm}_{j\bar 1} \tag{B.9}$$

$$K^{\pm}_{\bar 1 j} = \frac{d\theta}{2\pi}\frac{\phi^{\pm}_{\bar 1 j}}{1+e^{\epsilon_j}} \quad ; \qquad K^{\pm}_{ij} = \frac{d\theta}{2\pi}\frac{\phi^{\pm}_{ij}}{1+e^{\epsilon_j}} \tag{B.10}$$

Here $\partial\epsilon_{\bar 1} = \partial_\theta\epsilon|_{\theta=\theta_{\bar 1}}$. In calculating this expression we take the derivative of the TBA equation wrt. θ:

$$\partial_\theta\epsilon(\theta) = mL\sinh\theta + i(\phi(\theta-\bar\theta_1) - \phi(\theta+\bar\theta_1) + \int_{-\infty}^{\infty}\frac{d\theta'}{2\pi}\frac{\phi(\theta-\theta')}{1+e^{\epsilon(\theta')}}\partial_{\theta'}\epsilon(\theta') \tag{B.11}$$

Thus in our discretized formulation

$$\partial\epsilon_j = (\mathbb{I}-K)^{-1}_{jk}(mL\sinh\theta_k + i\phi^{-}_{k\bar 1}) \tag{B.12}$$

$$\partial\epsilon_{\bar 1} = mL\sinh\theta_{\bar 1} + i\phi^{-}_{\bar 1\bar 1} + K_{\bar 1 j}\partial\epsilon_j$$

where $K_{ij} = \frac{d\theta}{2\pi}\frac{\phi_{ij}}{1+e^{\epsilon_j}}$ acts on the whole line. The contribution of the determinants is the same as before except we replace $K^{\pm}$ with $K^{\pm}_{\rm ex}$. Thus the final results for the excited state g-function are

$$\log g^{\rm ex}_\alpha = -\frac{1}{4}\log(1+e^{-\epsilon_{i0}}) + \frac{d\theta}{4\pi}\sum_i(\phi_\alpha(\theta_i) - \phi(2\theta_i))\log(1+e^{-\epsilon_i}) \tag{B.13}$$

$$+\frac{1}{2}\left(\log\det(\mathbb{I}-K^{-}_{\rm ex}) - \log\det(\mathbb{I}-K^{+}_{\rm ex})\right) + \log\frac{R_{\mathbb{I}}(\theta_{\bar 1})}{\sqrt{S(2\theta_{\bar 1})}}$$

In case of a boundary boundstate at iu we add a term

$$\log(1+e^{-\epsilon_u}) \quad ; \qquad \epsilon_u = mL\cos u + \log\frac{S(iu-\theta_{\bar{1}})}{S(iu+\theta_{\bar{1}})} - \sum_j \phi(iu-\theta_j)\log(1+e^{-\epsilon_j}) \tag{B.14}$$

References

[1] M. de Leeuw, C. Kristjansen, K. Zarembo, One-point functions in defect CFT and integrability, J. High Energy Phys. 08 (2015) 098, https://doi.org/10.1007/JHEP08(2015)098, arXiv:1506.06958.

[2] I. Buhl-Mortensen, M. de Leeuw, C. Kristjansen, K. Zarembo, One-point functions in AdS/dCFT from matrix product states, J. High Energy Phys. 02 (2016) 052, https://doi.org/10.1007/JHEP02(2016)052, arXiv:1512.02532.

[3] M. De Leeuw, C. Kristjansen, G. Linardopoulos, Scalar one-point functions and matrix product states of AdS/dCFT, Phys. Lett. B 781 (2018) 238–243, https://doi.org/10.1016/j.physletb.2018.03.083, arXiv:1802.01598.

[4] M. de Leeuw, C. Kristjansen, G. Linardopoulos, One-point functions of non-protected operators in the SO(5) symmetric D3–D7 dCFT, J. Phys. A 50 (25) (2017) 254001, https://doi.org/10.1088/1751-8121/aa714b, arXiv:1612.06236.

[5] M. De Leeuw, T. Gombor, C. Kristjansen, G. Linardopoulos, B. Pozsgay, Spin chain overlaps and the twisted Yangian, J. High Energy Phys. 01 (2020) 176, https://doi.org/10.1007/JHEP01(2020)176, arXiv:1912.09338.

[6] I. Buhl-Mortensen, M. de Leeuw, A.C. Ipsen, C. Kristjansen, M. Wilhelm, One-loop one-point functions in gauge-gravity dualities with defects, Phys. Rev. Lett. 117 (23) (2016) 231603, https://doi.org/10.1103/PhysRevLett.117.231603, arXiv:1606.01886.

[7] I. Buhl-Mortensen, M. de Leeuw, A.C. Ipsen, C. Kristjansen, M. Wilhelm, Asymptotic one-point functions in gauge-string duality with defects, Phys. Rev. Lett. 119 (26) (2017) 261604, https://doi.org/10.1103/PhysRevLett.119.261604, arXiv:1704.07386.

[8] G. Linardopoulos, Solving holographic defects, PoS CORFU2019 (2019) 141, arXiv:2005.02117.

[9] C. Kristjansen, D. Müller, K. Zarembo, Integrable boundary states in D3-D5 dCFT: beyond scalars, J. High Energy Phys. 08 (2020) 103, https://doi.org/10.1007/JHEP08(2020)103, arXiv:2005.01392.

[10] T. Gombor, Z. Bajnok, Boundary states, overlaps, nesting and bootstrapping AdS/dCFT, J. High Energy Phys. 10 (2020) 123, https://doi.org/10.1007/JHEP10(2020)123, arXiv:2004.11329.

[11] T. Gombor, Z. Bajnok, Boundary state bootstrap and asymptotic overlaps in AdS/dCFT, arXiv:2006.16151.

[12] S. Komatsu, Y. Wang, Non-perturbative defect one-point functions in planar $\mathcal{N}=4$ super-Yang-Mills, Nucl. Phys. B 958 (2020) 115120, https://doi.org/10.1016/j.nuclphysb.2020.115120, arXiv:2004.09514.

[13] Y. Jiang, S. Komatsu, E. Vescovi, Structure constants in $\mathcal{N}=4$ SYM at finite coupling as worldsheet g-function, J. High Energy Phys. 07 (07) (2020) 037, https://doi.org/10.1007/JHEP07(2020)037, arXiv:1906.07733.

[14] Y. Jiang, S. Komatsu, E. Vescovi, Exact three-point functions of determinant operators in planar $N=4$ super-symmetric Yang-Mills theory, Phys. Rev. Lett. 123 (19) (2019) 191601, https://doi.org/10.1103/PhysRevLett.123.191601, arXiv:1907.11242.

[15] J.-S. Caux, F.H. Essler, Time evolution of local observables after quenching to an integrable model, Phys. Rev. Lett. 110 (25) (2013) 257203, https://doi.org/10.1103/PhysRevLett.110.257203, arXiv:1301.3806.

[16] K. Kozlowski, B. Pozsgay, Surface free energy of the open XXZ spin-1/2 chain, J. Stat. Mech. 1205 (2012) P05021, https://doi.org/10.1088/1742-5468/2012/05/P05021, arXiv:1201.5884.

[17] M. Brockmann, J. De Nardis, B. Wouters, J.-S. Caux, A Gaudin-like determinant for overlaps of Neel and XXZ Bethe states, J. Phys. A, Math. Theor. 47 (14) (2014) 145003, https://doi.org/10.1088/1751-8113/47/14/145003.

[18] B. Pozsgay, Overlaps with arbitrary two-site states in the XXZ spin chain, J. Stat. Mech. 1805 (5) (2018) 053103, https://doi.org/10.1088/1742-5468/aabbe1, arXiv:1801.03838.

[19] L. Piroli, B. Pozsgay, E. Vernier, What is an integrable quench?, Nucl. Phys. B 925 (2017) 362–402, https://doi.org/10.1016/j.nuclphysb.2017.10.012, arXiv:1709.04796.

[20] L. Piroli, E. Vernier, P. Calabrese, B. Pozsgay, Integrable quenches in nested spin chains I: the exact steady states, J. Stat. Mech. 1906 (6) (2019) 063103, https://doi.org/10.1088/1742-5468/ab1c51, arXiv:1811.00432.

[21] L. Piroli, E. Vernier, P. Calabrese, B. Pozsgay, Integrable quenches in nested spin chains II: fusion of boundary transfer matrices, J. Stat. Mech. 1906 (6) (2019) 063104, https://doi.org/10.1088/1742-5468/ab1c52, arXiv:1812.05330.

[22] D. Horvath, S. Sotiriadis, G. Takacs, Initial states in integrable quantum field theory quenches from an integral equation hierarchy, Nucl. Phys. B 902 (2016) 508–547, https://doi.org/10.1016/j.nuclphysb.2015.11.025, arXiv:1510.01735.
[23] D. Horvath, G. Takacs, Overlaps after quantum quenches in the sine-Gordon model, Phys. Lett. B 771 (2017) 539–545, https://doi.org/10.1016/j.physletb.2017.05.087, arXiv:1704.00594.
[24] D. Horvath, M. Kormos, G. Takacs, Overlap singularity and time evolution in integrable quantum field theory, J. High Energy Phys. 08 (2018) 170, https://doi.org/10.1007/JHEP08(2018)170, arXiv:1805.08132.
[25] T. Rakovszky, M. Mestyan, M. Collura, M. Kormos, G. Takacs, Hamiltonian truncation approach to quenches in the Ising field theory, Nucl. Phys. B 911 (2016) 805–845, https://doi.org/10.1016/j.nuclphysb.2016.08.024, arXiv:1607.01068.
[26] K. Hodsagi, M. Kormos, G. Takacs, Perturbative post-quench overlaps in quantum field theory, J. High Energy Phys. 08 (2019) 047, https://doi.org/10.1007/JHEP08(2019)047, arXiv:1905.05623.
[27] M. Kormos, B. Pozsgay, One-point functions in massive integrable QFT with boundaries, J. High Energy Phys. 04 (2010) 112, https://doi.org/10.1007/JHEP04(2010)112, arXiv:1002.2783.
[28] G. Takacs, G. Watts, Excited state G-functions from the truncated conformal space, J. High Energy Phys. 02 (2012) 082, https://doi.org/10.1007/JHEP02(2012)082, arXiv:1112.2906.
[29] P. Dorey, A. Pocklington, R. Tateo, G. Watts, TBA and TCSA with boundaries and excited states, Nucl. Phys. B 525 (1998) 641–663, https://doi.org/10.1016/S0550-3213(98)00339-3, arXiv:hep-th/9712197.
[30] P. Dorey, I. Runkel, R. Tateo, G. Watts, g function flow in perturbed boundary conformal field theories, Nucl. Phys. B 578 (2000) 85–122, https://doi.org/10.1016/S0550-3213(99)00772-5, arXiv:hep-th/9909216.
[31] M. Luscher, Volume dependence of the energy spectrum in massive quantum field theories. 1. Stable particle states, Commun. Math. Phys. 104 (1986) 177, https://doi.org/10.1007/BF01211589.
[32] M. Luscher, Volume dependence of the energy spectrum in massive quantum field theories. 2. Scattering states, Commun. Math. Phys. 105 (1986) 153–188, https://doi.org/10.1007/BF01211097.
[33] Z. Bajnok, R.A. Janik, Four-loop perturbative Konishi from strings and finite size effects for multiparticle states, Nucl. Phys. B 807 (2009) 625–650, https://doi.org/10.1016/j.nuclphysb.2008.08.020, arXiv:0807.0399.
[34] A. Zamolodchikov, Thermodynamic Bethe ansatz in relativistic models. Scaling three state Potts and Lee-Yang models, Nucl. Phys. B 342 (1990) 695–720, https://doi.org/10.1016/0550-3213(90)90333-9.
[35] P. Dorey, R. Tateo, Excited states by analytic continuation of TBA equations, Nucl. Phys. B 482 (1996) 639–659, https://doi.org/10.1016/S0550-3213(96)00516-0, arXiv:hep-th/9607167.
[36] I. Affleck, A.W. Ludwig, Universal noninteger 'ground state degeneracy' in critical quantum systems, Phys. Rev. Lett. 67 (1991) 161–164, https://doi.org/10.1103/PhysRevLett.67.161.
[37] D. Friedan, A. Konechny, On the boundary entropy of one-dimensional quantum systems at low temperature, Phys. Rev. Lett. 93 (2004) 030402, https://doi.org/10.1103/PhysRevLett.93.030402, arXiv:hep-th/0312197.
[38] A. LeClair, G. Mussardo, H. Saleur, S. Skorik, Boundary energy and boundary states in integrable quantum field theories, Nucl. Phys. B 453 (1995) 581–618, https://doi.org/10.1016/0550-3213(95)00435-U, arXiv:hep-th/9503227.
[39] F. Woynarovich, O(1) contribution of saddle point fluctuations to the free energy of Bethe ansatz systems, Nucl. Phys. B 700 (2004) 331–360, https://doi.org/10.1016/j.nuclphysb.2004.08.043, arXiv:cond-mat/0402129.
[40] P. Dorey, D. Fioravanti, C. Rim, R. Tateo, Integrable quantum field theory with boundaries: the exact g function, Nucl. Phys. B 696 (2004) 445–467, https://doi.org/10.1016/j.nuclphysb.2004.06.045, arXiv:hep-th/0404014.
[41] B. Pozsgay, On O(1) contributions to the free energy in Bethe ansatz systems: the exact g-function, J. High Energy Phys. 08 (2010) 090, https://doi.org/10.1007/JHEP08(2010)090, arXiv:1003.5542.
[42] I. Kostov, D. Serban, D.-L. Vu, Boundary TBA, trees and loops, Nucl. Phys. B 949 (2019) 114817, https://doi.org/10.1016/j.nuclphysb.2019.114817, arXiv:1809.05705.
[43] I. Kostov, Effective quantum field theory for the thermodynamical Bethe ansatz, J. High Energy Phys. 02 (2020) 043, https://doi.org/10.1007/JHEP02(2020)043, arXiv:1911.07343.
[44] S. Ghoshal, A.B. Zamolodchikov, Boundary S matrix and boundary state in two-dimensional integrable quantum field theory, Int. J. Mod. Phys. A 9 (1994) 3841–3886, https://doi.org/10.1142/S0217751X94001552; Int. J. Mod. Phys. A 9 (1994) 4353 (Erratum), arXiv:hep-th/9306002.
[45] J.L. Cardy, G. Mussardo, S matrix of the Yang-Lee edge singularity in two-dimensions, Phys. Lett. B 225 (1989) 275–278, https://doi.org/10.1016/0370-2693(89)90818-6.
[46] P. Dorey, R. Tateo, G. Watts, Generalizations of the Coleman-Thun mechanism and boundary reflection factors, Phys. Lett. B 448 (1999) 249–256, https://doi.org/10.1016/S0370-2693(99)00004-0, arXiv:hep-th/9810098.
[47] Z. Bajnok, L. Palla, G. Takacs, Boundary one-point function, Casimir energy and boundary state formalism in D+1 dimensional QFT, Nucl. Phys. B 772 (2007) 290–322, https://doi.org/10.1016/j.nuclphysb.2007.02.023, arXiv:hep-th/0611176.

[48] Z. Bajnok, L. Palla, G. Takacs, Finite size effects in quantum field theories with boundary from scattering data, Nucl. Phys. B 716 (2005) 519–542, https://doi.org/10.1016/j.nuclphysb.2005.03.021, arXiv:hep-th/0412192.
[49] Z. Bajnok, L. Palla, G. Takacs, On the boundary form-factor program, Nucl. Phys. B 750 (2006) 179–212, https://doi.org/10.1016/j.nuclphysb.2006.05.019, arXiv:hep-th/0603171.
[50] B. Pozsgay, G. Takacs, Form factors in finite volume. II. Disconnected terms and finite temperature correlators, Nucl. Phys. B 788 (2008) 209–251, https://doi.org/10.1016/j.nuclphysb.2007.07.008, arXiv:0706.3605.
[51] B. Pozsgay, G. Takacs, Form-factors in finite volume I: form-factor bootstrap and truncated conformal space, Nucl. Phys. B 788 (2008) 167–208, https://doi.org/10.1016/j.nuclphysb.2007.06.027, arXiv:0706.1445.
[52] Y. Jiang, B. Pozsgay, On exact overlaps in integrable spin chains, J. High Energy Phys. 06 (2020) 022, https://doi.org/10.1007/JHEP06(2020)022, arXiv:2002.12065.
[53] F. Woynarovich, On the normalization of the partition function of Bethe ansatz systems, Nucl. Phys. B 852 (2011) 269–286, https://doi.org/10.1016/j.nuclphysb.2011.06.015, arXiv:1007.1148.
[54] Z. Bajnok, F. Smirnov, Diagonal finite volume matrix elements in the sinh-Gordon model, Nucl. Phys. B 945 (2019) 114664, https://doi.org/10.1016/j.nuclphysb.2019.114664, arXiv:1903.06990.
[55] Z. Bajnok, I. Vona, Exact finite volume expectation values of conserved currents, Phys. Lett. B 805 (2020) 135446, https://doi.org/10.1016/j.physletb.2020.135446, arXiv:1911.08525.
[56] V. Yurov, A. Zamolodchikov, Truncated conformal space approach to scaling Lee-Yang model, Int. J. Mod. Phys. A 5 (1990) 3221–3246, https://doi.org/10.1142/S0217751X9000218X.
[57] M. Kormos, G. Takacs, Boundary form-factors in finite volume, Nucl. Phys. B 803 (2008) 277–298, https://doi.org/10.1016/j.nuclphysb.2008.05.003, arXiv:0712.1886.
[58] M. Lencses, G. Takacs, Breather boundary form factors in sine-Gordon theory, Nucl. Phys. B 852 (2011) 615–633, https://doi.org/10.1016/j.nuclphysb.2011.07.010, arXiv:1106.1902.
[59] J.L. Cardy, Boundary conditions, fusion rules and the Verlinde formula, Nucl. Phys. B 324 (1989) 581–596, https://doi.org/10.1016/0550-3213(89)90521-X.
[60] A. Konechny, RG boundaries and interfaces in Ising field theory, J. Phys. A 50 (14) (2017) 145403, https://doi.org/10.1088/1751-8121/aa60f6, arXiv:1610.07489.
[61] Z. Bajnok, M. Lajer, B. Szepfalvi, I. Vona, Leading exponential finite size corrections for non-diagonal form factors, J. High Energy Phys. 07 (2019) 173, https://doi.org/10.1007/JHEP07(2019)173, arXiv:1904.00492.
[62] R. Konik, M. Lájer, G. Mussardo, Approaching the self-dual point of the sinh-Gordon model, J. High Energy Phys. 01 (2021) 014, https://doi.org/10.1007/JHEP01(2021)014, arXiv:2007.00154.
[63] J.a. Caetano, S. Komatsu, Functional equations and separation of variables for exact g-function, J. High Energy Phys. 09 (2020) 180, https://doi.org/10.1007/JHEP09(2020)180, arXiv:2004.05071.
[64] D.-L. Vu, I. Kostov, D. Serban, Boundary entropy of integrable perturbed SU $(2)_k$ WZNW, J. High Energy Phys. 08 (2019) 154, https://doi.org/10.1007/JHEP08(2019)154, arXiv:1906.01909.
[65] T. Gombor, Nonstandard Bethe ansatz equations for open O(N) spin chains, Nucl. Phys. B 935 (2018) 310–343, https://doi.org/10.1016/j.nuclphysb.2018.08.014, arXiv:1712.03753.
[66] Z. Bajnok, J.L. Jacobsen, Y. Jiang, R.I. Nepomechie, Y. Zhang, Cylinder partition function of the 6-vertex model from algebraic geometry, J. High Energy Phys. 06 (2020) 169, https://doi.org/10.1007/JHEP06(2020)169, arXiv:2002.09019.